Elsevier Editorial System(tm) for Marine Chemistry
Manuscript Draft

Manuscript Number: MARCHE-D-14-00212R2

Title: Atmospheric trace metal concentrations, solubility and deposition fluxes in remote marine air over the south-east Atlantic

Article Type: SI: Ocean Biogeochemistry

Keywords: Aerosols; Atmospheric deposition; Trace metals; Solubility; Atlantic Ocean; GEOTRACES

Corresponding Author: Dr. Rosie Chance,

Corresponding Author's Institution: University of York

First Author: Rosie Chance

Order of Authors: Rosie Chance; Tim D Jickells; Alex R Baker

Manuscript Region of Origin:

Abstract: Total and soluble trace metal concentrations were determined in atmospheric aerosol and rainwater samples collected during seven cruises in the south-east Atlantic. Back trajectories indicated the samples all represented remote marine air masses, consistent with climatological expectations. Aerosol trace metal loadings were similar to previous measurements in clean, marine air masses. Median total Fe, Al, Mn, V, Co and Zn concentrations were 206, 346, 5, 3, 0.7 and 11 pmol m-3 respectively. Solubility was operationally defined as the fraction extractable using a pH4.7 ammonium acetate leach. Median soluble Fe, Al, Mn, V, Co, Zn, Cu, Ni, Cd and Pb concentrations were 6, 55, 1, 0.7, 0.06, 24, 2, 1, 0.05 and 0.3 pmol m-3 respectively. Large ranges in fractional solubility were observed for all elements except Co; median solubility values for Fe, Al and Mn were below 20% while the median for Zn was 74%. Volume weighted mean rainwater concentrations were 704, 792, 32, 10, 3, 686, 25, 0.02, 0.3 and 10 nmol L-1 for Fe, Al, Mn, V, Co, Zn, Cu, Ni, Cd and Pb respectively (n = 6). Wet deposition fluxes calculated from these values suggest rain makes a significant contribution to total deposition in the study area for all elements except perhaps Ni.

Responses to Reviewers MARCHE-D-14-00212R1

Line and page numbers refer to manuscript R1

Reviewer #1

This is my second reading of this manuscript and it is much improved in the current form. The authors rightfully point out that this dataset, while limited in size, is a valuable contribution to our understanding of aerosol chemistry and deposition in the study region. The authors have addressed many of my initial comments and strengthened the interpretation of their data. Some issues that I and the other reviewers raised, such as the small sample sizes, methodology, etc., remain but should not preclude publication in my opinion. I do believe that the following points warrant consideration.

We thank Reviewer#1 for these supportive comments, and for their two reviews, which have improved our manuscript.

My greatest reservation is regarding both wet and dry flux estimation. For the former, the very few observations are likely not representative, as acknowledged by the authors. My concern is that the data will not ultimately be of much value to the larger community for this reason but I also recognize the paucity of observations in the literature and fully acknowledge that some data is better than no data. However, I do not think that the claim of 90% wet deposition can be substantiated based on the data provided. I recommend that the authors reconsider this statement in light of having made only six observations of wet deposition.

We have deleted this statement from Section 3.6 (P21, L9). The wording of this paragraph has also been slightly rearranged and reworded to emphasise that our deposition fluxes are only estimates and are subject to large uncertainties. We already noted (P21, L33) that "due to the large uncertainty associated with the wet deposition flux estimates (Table 5), it is not possible to conclude definitively that wet deposition is the dominant term" - this statement has been moved further up the paragraph to emphasise this point.

We would like to highlight that, although our results are subject to substantial uncertainty, particularly due to the small number of rain samples, the finding that wet is the dominant contributor to total deposition is consistent with other studies, as described in the text (P21, L13, L18 & L24).

The high levels of uncertainty associated with our estimates of wet deposition are already revisited in our conclusions (Section 4). We have inserted the phrase "our estimates of" before "total (wet plus dry) deposition" (P23, L22) as a further reminder of the limitations of our data, and replaced the phrase "Given the substantial contribution of wet deposition...," with "Given there appears to be a substantial contribution of wet deposition...." later in the paragraph. (P23, L29)

The final sentence of the abstract (P1, L54) has also been reworded to reflect Reviewer #1's concern, and the number of rainwater samples has been added to the abstract to make clear the small sample size.

The authors spend a great deal of time discussing the choice of deposition velocity in dry deposition calculations as it pertains to particle size and uncertainty in deposition rate. However, I don't think that the size distribution is effectively characterized by the few samples collected. This section could be simplified and shortened by choosing
a single deposition velocity. The variability in aerosol concentration driven by the well characterized episodic nature of aerosol emission and transport over long time scales is a more likely source of differences in flux than the choice of deposition velocity applied to short term shipboard collections.

We agree with Reviewer#1 that we only have limited information concerning size distribution. Consequently, we do present dry deposition fluxes calculated using a single value of deposition velocity (V_d; see Section 2.3 and Table 4). In our original manuscript, we only presented these results - deposition fluxes calculated using larger (for lithogenic elements) and smaller (for anthropogenic elements) values of V_d were added to the revised manuscript in response to comments from reviewer#2 and #3 in the initial manuscript reviews.

The inclusion of fluxes calculated using alternative V_d values was intended to help quantify the uncertainty arising from this parameter, as this was a major concern of the original reviewers. A brief phrase explaining our approach has been added to Section 2.3. We feel that by attempting to address the uncertainty in V_d, we are better able to consider variation from other sources, such as those suggested by Reviewer#1. Related to this, our approach allows more direct comparison with other reported deposition fluxes, which use various V_d values (see Section 3.5). As discussed in the text, this treatment does not substantially alter our conclusions.

Given the requests from the other reviewers for expansion of our discussion of this topic from that in the earlier version of our paper, we have decided against shortening it again as Reviewer #1 suggests here.

The authors report a majority of soluble Fe, Al and Mn in the coarse size fraction. It is a pity that total aerosol concentration was not measured on the size fractionated samples to determine if this is a function of solubility or just loading. Are there other published datasets of size fractionated aerosols from the Atlantic to offer some comparison?

We have added the following comments regarding published values of total trace metal size distribution.

P13, L2: "Previous studies of the aerosol size distribution in Atlantic remote marine air masses have tended to find the majority of total Fe to reside in the coarse mode: ~64%, ~67% and ~70% of total Fe was found in the coarse mode in samples collected in the south-west Atlantic (Baker et al., 2006a), the tropical Atlantic

(Baker et al., 2006b) and the north Atlantic (~17°N; Fomba et al., 2013) respectively. However, ~65% of total Fe was found in the fine mode in a single south Atlantic sample (~11-14°S; Radlein and Heumann, 1995), suggesting variation in the total Fe size distribution can occur. Similarly, the fraction of total Mn in the coarse mode has been reported as ~74% in the south-west Atlantic (Baker et al., 2006a) and ~70% in the tropical Atlantic (Baker et al., 2006b), but only ~50% in remote marine air in the north Atlantic (Fomba et al., 2013). As the size distributions of total metals were not determined in our study, it is not possible to conclude whether the soluble distribution is a function of the total metal distribution, the metal solubility, or both."

P13, L55: "A similar predominance of total V in the fine aerosol mode (~70%) has been observed in remote north Atlantic air masses (Fomba et al., 2013), suggesting the soluble size distribution we observe reflects the total V distribution."

P14, L49: "Previous measurements of Atlantic remote marine aerosols have found that total Zn, Cu and Pb are also predominantly found in the fine mode (Radlein & Heumann 1995; Fomba et al., 2013)."

P14, L51: "Previous studies in similar air masses have found the majority (~70% or more) of total Cd and Ni resides in the fine mode (Radlein & Heumann 1995; Fomba et al., 2013), with this distribution appearing to be ubiquitous for total Cd (Radlein & Heumann 1995). In this case, the variation in soluble size distribution we observe may reflect differences in solubility between the size fractions, rather than variation in total metal loading."

In the interests of brevity, we have not commented on every element.

References for Fomba et al. 2013, and Baker et al., 2006b have been added to the References.

The authors observe higher solubility in "southerly" samples attributing this to enhanced atmospheric processing within these air masses. Setting aside concerns over the uncertainty in 5 day AMBTs, is this reasonable? These southerly samples could be influenced by continental sources in South America which extends at least as far south as 55o. Also, there is little to no industrial activity in the region greatly reducing the availability of acidic precursor by which to process the aerosols. Further, recent work in the North Pacific reported that aerosol Fe did not increase in solubility between Asia and North America (Buck, C.S., W.M. Landing, J. Resing. Pacific Ocean Aerosols: Deposition and Solubility of Iron, Aluminum, and Other Trace Elements (2013). Mar. Chem., 157, 117-130, doi:10.1016/j.marchem.2013.09.005).

In light of Reviewer#1's comments we have rewritten the paragraph as follows:

P15, L51 - P16, L4: "There are a number of potential causes of this apparent solubility gradient (e.g. higher solubility in more southerly dust sources, longer periods of atmospheric processing in the more southerly samples, differences in

aerosol pH due to latitudinal variation in gaseous emissions), and we are not able to identify which of these processes is responsible here. It is also possible that systematic biases, for example seasonality in aerosol sources, transport and/or processing, may have caused this apparent spatial divide, as all southerly samples were collected during the Z-D and BGH cruises. Recent work in the Pacific has found that aerosol Fe solubility does not increase with distance from source (Buck et al., 2013); further work is needed to improve understanding of spatial variation in trace metal solubility."

The reference for Buck et al. 2013, has been added to the References.

The authors suggest seasonal differences among the cruises as an alternative explanation but do not elaborate. Are they suggesting seasonal differences in aerosol
source, transport or some other mechanism? This point needs clarification.

We do not have sufficient information to identify specific seasonal factors. Therefore we have indicated that the possible seasonality may apply to "aerosol sources, transport and/or processing" (P16, L1 - see above).

Reviewer #2

Authors have addressed all my comments.

We are pleased that Reviewer#2 is satisfied with our changes, and thank them for their reviews, which have improved our manuscript.

Fig. 4 and Fig. 6: The titles of Y-axis are missing.

Y-axis titles have been added to Figs. 4 and 6

Fig. 7: The titles of both X-axis and Y-axis are missing.

X- and Y-axis titles have been added to Fig. 7B.

Page 16: It is interesting that the cluster of samples with high Mn concentrations, low solubiliy and high EF values are all collected in the East of 0 degree, which should be indicated in the text and may help explain the behavior of Mn.

We have added the following sentence:

P16, L48: "They tended to occur to the east of the sampling region (Supplementary information, Figs S1, S2 and S3), and most, but not all, were collected during cruise D357."

Atmospheric trace metal concentrations, solubility and deposition fluxes in remote marine air over the south-east Atlantic

Rosie Chance[a,*], *Timothy D. Jickells*[a], *Alex R. Baker*[a],

a. Centre for Ocean and Atmospheric Sciences, School of Environmental Sciences, University of East Anglia, Norwich, NR4 7TJ, UK.

** Corresponding author. Current address: Wolfson Atmospheric Chemistry Laboratory, Department of Chemistry, University of York, YO10 4DD, UK.*

Email address: rosie.chance@york.ac.uk

Keywords: Aerosols; Atmospheric deposition; Trace metals; Solubility; Atlantic Ocean; GEOTRACES

Abstract

Total and soluble trace metal concentrations were determined in atmospheric aerosol and rainwater samples collected during seven cruises in the south-east Atlantic. Back trajectories indicated the samples all represented remote marine air masses, consistent with climatological expectations. Aerosol trace metal loadings were similar to previous measurements in clean, marine air masses. Median total Fe, Al, Mn, V, Co and Zn concentrations were 206, 346, 5, 3, 0.7 and 11 pmol m^{-3} respectively. Solubility was operationally defined as the fraction extractable using a pH4.7 ammonium acetate leach. Median soluble Fe, Al, Mn, V, Co, Zn, Cu, Ni, Cd and Pb concentrations were 6, 55, 1, 0.7, 0.06, 24, 2, 1, 0.05 and 0.3 pmol m^{-3} respectively. Large ranges in fractional solubility were observed for all elements except Co; median solubility values for Fe, Al and Mn were below 20% while the median for Zn was 74%. Volume weighted mean rainwater concentrations were 704, 792, 32, 10, 3, 686, 25, 0.02, 0.3 and 10 nmol L^{-1} for Fe, Al, Mn, V, Co, Zn, Cu, Ni, Cd and Pb respectively (n = 6). Wet deposition fluxes calculated from these values suggest rain makes a significant contribution to total deposition in the study area for all elements except perhaps Ni.

1. Introduction

The transport and deposition of atmospheric aerosol is a significant source of trace metals to the surface ocean (Jickells et al., 2005), and in large areas of the open ocean may represent the dominant supply route for certain elements (Ussher et al., 2013). A range of trace metals (e.g. Fe, Zn, Co) are required for phytoplankton growth, and their availability is limiting or co-limiting in some ocean regions (Saito et al., 2008; Dixon, 2008; Moore et al., 2013). Consequently, the supply of micronutrients to the surface ocean impacts on primary productivity, and thus the potential of the oceans to sequester carbon (e.g. Cassar et al., 2007). In addition to direct impacts on phytoplankton growth, micronutrient availability may also influence functioning of the marine ecosystem via indirect mechanisms, particularly via impacts on nitrogen fixation (Moore et al., 2009; 2013). Another example of an indirect impact is the use of Co by marine prokaryotes in the synthesis of vitamin B12, an exogenous supply of which is required by eukaryotic phytoplankton (Panzeca et al., 2008). Some trace elements present in atmospheric deposition, for example Cu, can also be toxic to marine organisms (Paytan et al., 2009; Jordi et al., 2012).

Micronutrient levels are low in both the oligotrophic subtropical waters of the south Atlantic gyre, and the high nutrient - low chlorophyll waters of the Southern Ocean. Consequently, biogeochemical cycles in both regions are sensitive to atmospheric dust inputs (Cassar et al., 2007; Dixon, 2008). The south Atlantic receives lower atmospheric inputs than the equatorial and northern Atlantic (Sarthou et al., 2003; Ussher et al., 2013). Despite these lower inputs, atmospheric deposition still accounts for more than 50% of the vertical inputs of iron to the surface mixed layer, with the remainder supplied by mixing from below (Ussher et al., 2013). As westerly winds predominate, aeolian and volcanic dust originating in southern South America is considered to be main source of dust inputs to the south Atlantic (Gaiero et al., 2004; Li et al., 2008; Johnson et al., 2010).

Despite several decades of research, the atmospheric deposition of trace metals to the oceans is not well quantified. Atmospheric loadings of trace metals over the oceans display high variability, reflecting the diversity of source regions and the episodic nature of sources such as dust mobilisation. Understanding the impact of atmospheric deposition on the south

Atlantic and Southern Ocean requires improvements in the characterisation of atmospheric trace element (particularly elements other than Fe, Al, Mn) concentrations from sources such as South America (Johnson et al., 2010; Schulz et al., 2012). There is also a need for more information on the solubility and size distribution of aerosol trace metals, in order to better parameterise models (Mahowald et al., 2009; Schulz et al., 2012; Baker et al., 2013).

The aim of this work was to present representative atmospheric aerosol and rain water concentrations for the south-east Atlantic, and use these measurements to estimate atmospheric deposition fluxes to the region. A suite of ten elements is included for soluble metal concentrations, and six for total metal concentrations. The data used here comes from four cruises which are previously unpublished (D357 and JC068) or for which only a limited selection of data has been published previously (BGH and ZD; Sholkovitz et al., 2012; Boye et al., 2012; Bown et al., 2011). We also make use of aerosol data for Fe, Al and Mn from three other cruises (AMT15, AMT16 and AMT17; Baker et al., 2013), to provide a detailed study of this historically under-sampled region. We believe the aerosol and rain trace metal concentrations measured on these seven cruises comprise the most extensive data set for the region currently available. The results presented here are intended as a contribution to the growing global database of marine aerosol measurements, and were obtained under the UK-GEOTRACES research programme.

2. Methods

2.1. Sample collection

Atmospheric aerosol and rainwater samples were collected during seven research cruises that took place between 2004 and 2012. Aerosol sampling mid-points are shown in Fig. 1 and rain sample locations are shown in Fig. 2; further details of the cruises are given in Table 1. The dominant wind direction over the sampling region is from the west/northwest (Barry & Chorley, 1971), so atmospheric deposition to these surface waters likely originated in South America rather than southern Africa. With the exception of AMT16, which took place in May, sampling was conducted during the austral summer (October to March), and in general each cruise took place in a different month.

Atmospheric aerosol was collected using high volume Andersen samplers (flow rate of ~1 m^3 min^{-1}), mounted on the bridge-top deck of the ship. To avoid sampling contaminated air from

the ships funnel, the collectors were turned off when the ship was not facing into the wind or there was some other risk of contamination, such as testing of the lifeboat engines on the foredeck. During the more recent cruises (D357 and JC068), power supply to the motors was automatically controlled such that sampling only took place when the relative wind direction was between -80 and 145 degrees, thus avoiding the ships exhaust. Samples were collected over periods of ~24 or ~ 48 hours, depending on the anticipated aerosol loadings. Filter blanks and procedural blanks for the sampling cassette and the motor start up were collected. Bulk aerosol samples were collected using a single Whatman 41 filter paper, and size segregated aerosol samples were collected using a Sierra-type cascade impactor (fitted with two upper stages, with aerodynamic diameter cut-offs of ~2.4 and ~1.6 μm) onto slotted filters and a back-up filter behind (all Whatman 41). Occasionally, samples were collected using a six-stage impactor (also using Whatman 41 filters). Filters for trace metal determinations were washed in at least two consecutive acid baths before use. The filter washing procedures for individual cruises were as follows: AMT15, AMT17, D357, JC068 - HCl (0.5M) then HNO_3 (0.1M); AMT16 - HCl (0.5M) then HCl (0.1M); BGH, ZD - as for AMT16, then Suprapure HCl (0.1 M). The filters were loaded and unloaded from the sampling cassettes under a laminar flow hood; nitrile gloves were worn and the filters handled by the edges only. Exposed filters were folded in half, placed in sealed plastic bags and stored frozen at -20^{o}C until analysed in the UK.

Rainwater was collected using a 40 cm diameter polypropylene funnel with a clean sample bottle (250 or 500 mL) attached; a new bottle was used for each rain event. The bottles and funnel for trace metal clean rain sampling were acid washed and the bottles stored with 15.8 mM HNO_3 in them (Baker et al., 2007). The funnel was deployed on the bridge-top deck as close as possible to the start of a rain event, and removed as soon as possible after the rain ceased. Immediately prior to deployment, the funnel was rinsed with the dilute HNO_3 from the new sample bottle. Following collection, samples were acidified using concentrated HNO_3 (to a final concentration of 15.8 mM) and frozen at -20^{o}C for return to the UK. Blank samples were prepared by pouring the contents of a cleaned bottle (125 mL) through the funnel and into a second bottle. Details of the rain sampling events are given in Table S1 of the Supplementary information. No rain events were encountered in the study region during cruises AMT15, AMT16 and AMT17. Three precipitation samples were collected during the

BGH cruise, but all were found to be contaminated with soot from the ship's stack and so were not analysed. Rain sampling was not carried out during the ZD cruise.

2.2. Sample extraction and analysis

Total aerosol loadings of Fe, Al and Mn for all cruises were measured by instrumental neutron activation analysis (INAA), conducted at the SLOWPOKE nuclear reactor, École Polytechnique, Montreal, Canada. Additional elements were also measured in samples from cruises D357 (V, Co, Zn, Cu, Ni, Cd) and JC068 (V, Co, Zn only), though all total Cu, Cd and Ni measurements were below the limit of detection for the INAA protocol used. Total Pb could not be determined as part of the multi-element INAA method used here. Portions of filter samples (either bulk filters, or coarse and fine mode filters combined) in zip-lock polyethylene bags were placed in polyethylene irradiation vials and subject to a neutron flux of 5×10^{11} cm^2 s^{-1}. Gamma emission at element specific wavelengths was then used to quantify the elements of interest. Previous work has found no significant difference between total aerosol metal concentrations determined by INAA and strong acid digestion (Baker et al., 2013).

Soluble trace metals were operationally defined as those extracted using an established ammonium acetate (pH 4.7, 1.1 M) leach procedure (e.g. Baker et al., 2006, 2007). Portions of aerosol filter sample were immersed in the extraction solvent for one hour, with four intervals of manual shaking during this period. Extracts were then filtered (0.2 μm) into acid washed polypropylene sample tubes using disposable plastic syringe filters. All manipulations were conducted in a clean room and high purity reagents were used (Fluka Analytical Trace Select Ultra grade). Reagent blanks confirmed the extraction solvents and plastic ware did not cause contamination. Comparison of individual samples suggests that this method releases a greater fraction than ultrapure water leaches for some metals (Fe, Al, Pb), but is comparable for others (V) (Morton et al., 2013). Analysis of large data sets of Fe fractional solubility obtained using ammonium acetate and ultrapure water leaching indicate that the two methods give broadly similar results (Baker et al., 2014). The relevance of either of these leach protocols to trace metal dissolution in seawater is not yet established (see discussion in Baker and Croot, 2010).

Metal concentrations in aerosol sample extracts and acidified rainwater samples were measured using inductively coupled plasma - optical emission spectroscopy (ICP-OES; Fe,

Al, Mn, Zn, V) and inductively coupled plasma - mass spectrometry (ICP-MS; Co, Cd, Ni, Cu, Pb). Instrument responses were calibrated using matrix-matched solutions prepared from certified stock standards (Spex CertiPrep), and accuracy was checked using certified reference materials (CRMs; Environment Canada TMRAIN-04 and Fortified Water TM-27.3, purchased from LGC Ltd) and repeat analysis of in-house standard solutions. Analysis of CRM 'TMRAIN-04' (run alongside samples) yielded the following recoveries: >95% for Fe, Mn and Co, >90% for Ni and Cu, >85% for Pb, and >80% for V and Cd. Trace metal concentrations in CRM 'TMRAIN-04' were very low, being close to or below the limit of detection (LoD) in some cases, so was not suitable for determining accuracy for all elements, particularly Al, V, Pb, and Cd. Analysis of CRM 'TM-27.3', which has higher trace metal concentrations, gave a recovery of >90% for Al. Analytical errors were estimated from the standard error of the slope and intercept of the calibration curves, and propagated through to the final atmospheric concentrations.

2.3. Data processing

All sample concentrations were corrected using the procedural blanks. Samples were defined as being below the LoD according to two criteria: (i) those with extract concentrations below the analytical LoD, determined from the calibration curve, (ii) those with blank corrected values that were less than the procedural LoD, defined as 3 x standard deviation of the blank samples. LoD values are given in Table S2 (Supplementary information). Where samples were below either LoD, a value of 0.75 x LoD was substituted and the data point flagged. The limits of detection for total metals were typically at least an order of magnitude higher than for the soluble metal determinations, and hence a larger number of samples have been fully quantified for the latter. The proportion of samples that exceeded the LoD is given in Tables 2 and 3. Where either the total or soluble metal concentration was below the limit of detection, the sample was not included in calculations of solubility or size distribution.

Aerosol enrichment factors (EF) relative to crustal material were calculated according to equation (1),

$$EF = [X/Al]_{aerosol}/[X/Al]_{shale} \quad (1)$$

where $[X/Al]_{aerosol}$ is the molar ratio of element X to Al in aerosol, and $[X/Al]_{shale}$ is the elemental ratio in shale rock (Turekian and Wedepohl, 1961). Solubility was defined as 100

x ($C_{atm,\ soluble}$ / $C_{atm,\ total}$), where C_{atm} is the atmospheric concentration. In a few cases, soluble and total metal concentrations for a given sample and element yielded >100% solubility. Where this occurred the data was excluded from further analysis and is not presented below. Soluble V concentrations during cruise BGH, and soluble Cu and Cd measured during cruise ZD, were found to be extremely high relative to the rest of the data set (Fig S4, supplementary information). These data points were excluded from the calculation of summary statistics on the grounds that contamination during sampling was suspected. Other elements from these cruises were retained, as they were not significantly different to the remainder of the data set. This is discussed in Section 3.2.

Dry deposition fluxes (F_{dry}) were calculated using equation (2), where V_d is the deposition velocity. V_d is known to be dependent on wind speed and particle size (Slinn and Slinn, 1980), and remains a very large source of uncertainty in deposition flux calculations (Duce et al., 1991; Schulz et al., 2012). As the size distribution of total trace metal concentrations was not measured here we have used a single V_d value of 0.3 cm s^{-1} for all samples (Boye et al., 2012; Duce et al., 1991). In order to consider the impact of selected values of V_d, we have also calculated deposition fluxes using a larger V_d value of 1 cm s^{-1} for Fe, Al, Mn and Co, assuming these elements are associated with larger, mineral aerosol (Duce et al., 1991; Shelley et al., 2012; Baker et al., 2013), and a smaller V_d value of 0.03 cm s^{-1} for V, Zn, Cu, Ni, Cd and Pb, assuming they are associated with smaller, pollutant aerosol (Duce et al., 1991; Boye et al., 2012; Baker et al., 2013).

$$F_{dry} = C_{atm} \bullet V_d \qquad (2)$$

Wet deposition fluxes (F_{wet}) were calculated as the product of the volume weighted mean rainfall concentration (C_{rain}) and the average precipitation rate for the region (P) using equations 3 and 4, where C_i and V_i are the measured concentration and volume of rain collected for each sample.

$$C_{rain} = \Sigma C_i V_i / \Sigma V_i \qquad (3)$$

$$F_{wet} = C_{rain} \bullet P \qquad (4)$$

The precipitation rate (P) was taken as the area weighted average of long-term monthly mean rainfall for the months October to January (i.e. those during which the samples were

collected) and grid-points spanning 21.25 to 58.75°S, and 16.25°W to 21.25°E, see Fig. 2. CMAP Precipitation data was obtained from NOAA/OAR/ESRL PSD, Boulder, Colorado, USA, via the online portal at http://www.esrl.noaa.gov/psd/ (Xie, P., and P.A. Arkin, 1997).

2.4. Air mass origin

Five-day air mass back trajectories for each sample were produced using the HYSPLIT model provided by NOAA Air Resources Laboratory (Draxler and Rolph, http://www.arl.noaa.gov/HYSPLIT.php), using the model vertical velocity calculation method and GDAS1 meteorology. Trajectory arrival heights of 10, 500 and 1000 m above ground level were specified. Samples were assigned to different air mass source regions using the definitions described in earlier work (Baker et al., 2010; Baker et al., 2013).

3. Results and Discussion

3.1. Air mass origin

All but one of the samples collected in the study region (Fig. 1) had remote, marine source regions (Fig. 3), and are described as remote south Atlantic air using the terminology of previous work (Baker et al., 2013, 2010). The exception, (BGH-01), was collected close to South Africa and was categorised as a Southern African air mass. This sample had substantially higher metal loadings than the rest of the data set, and is excluded from further analysis here. Of the remaining samples, back trajectories suggested a further four were partially influenced by continental source regions in southern Africa (D357-15, JC068-04) or South America (D357-05, JC068-09), and three originated in Antarctica (D357-05, D357-11, ZD-04). Despite these continental influences, these samples were overall classified as remote marine air masses, and in general had trace metal loadings that fell within the range of the other samples.

The sampling area is approximately the same as the South Atlantic dry region (region 4d; see Fig. 1) defined by Baker et al. (2010; 2013) in their large-scale studies of N, Fe, Al and Mn deposition to the Atlantic. Baker et al. (2010; 2013) examined daily back trajectories arriving at a point location in this region (34°S, 12°E) over a five-year period. This point lies within our study region, close to the densest region of sampling points (see Fig. 1), and so we consider that the findings of Baker et al. (2010, 2013) regarding air mass origin are applicable

to our study. 93.3% of air masses arriving at this point in April, May and June, and 95.3% in September, October and November, are South Atlantic remote air (Baker et al., 2013), which has spent the preceding five days over the oceans, and similar proportions of remote marine air masses are expected in the intervening months. This is consistent with the vast majority of sample specific back trajectories for the samples discussed here being for remote marine air masses. Consequently, we believe the aerosol concentrations we report are representative of the area under typical conditions.

3.2. Total metal concentrations in aerosol

The majority of total Fe, Al and Mn concentrations (Table 2) fell within the ranges previously observed in the south Atlantic and Southern Ocean (Losno et al., 1992; Baker et al., 2013; Radlein and Heumann, 1992; Gao et al., 2013; see Table S3 in Supplementary information). No systematic spatial trends were evident in the total metal concentrations (see Supplementary information, Fig. S1), so only the summary statistics are considered further. The large range in the Fe data presented here arose from two samples with atypically high total Fe concentrations (ZD-01, D357-08), the remaining 37 samples had total iron loadings of less than 500 pmol m^{-3}. Note that even including these higher values, the range of total Fe concentrations is very small relative to global scale range, which spans ~four orders of magnitude (e.g. Sholkovitz et al., 2012; Baker et al., 2013). The absence of substantial variation between the samples is consistent with them all representing the same air mass type, and all being at least five days distant from relatively weak (on global scales) continental source regions (Section 3.1).

As for Fe, the range in total Al and Mn concentrations was small relative to that observed across the Atlantic Ocean (Baker et al., 2013). The Al values reported here tended to fall at the lower end of the reported ranges for remote marine air, with the exception of two very high concentration samples (ZD-01, ZD-02), which were outliers according to the Tukey definition (i.e. they were greater than 1.5 x the interquartile range plus the upper quartile). Although high relative to the remainder of this data set, these two Al concentrations (~7000 pmol m^{-3} total Al) are still at the lower end of that observed in the Atlantic (Baker et al., 2013), suggesting they are plausible. The source of the Al is not obvious, as neither the concentrations of other metals, or the back trajectories, distinguish these samples from the remainder. It is also possible that the high Al concentrations result from sample

contamination. Sample ZD-02 has Fe and Mn enrichment factors of less than 1, which could imply Al contamination specifically, but sample ZD-01 had Fe and Mn EF of about 1, suggesting the Al may be crustal in origin. As the Al concentrations in these two samples are still within realistic limits, and the cause of the elevated Al levels is unknown, the samples have been retained within the data set. Total Al and Mn concentrations were very similar to previously reported values for the south Atlantic (Baker et al., 2013; Völkening and Heumann 1990; Radlein and Heumann, 1995; see Table S3), and clean marine Pacific aerosol (Guieu et al., 1994; Table S3). The median total Al concentration was also strikingly similar to seasonal median concentrations reported by Baker et al., 2013 (363 pmol m^{-3} for April to June and 376 for September to November). Generally lower total Al concentrations were observed in marine aerosol collected on the Kerguelen Islands, in the Indian sector of the Southern Ocean (Heimburger et al., 2012; Table S3). These islands lie within the westerly circulation around the Southern Ocean and are recipients of South American dust (Li et al., 2008); the lower Al concentrations observed on Kerguelen may reflect their position downwind of our sampling region in the South American dust outflow.

Fe was only slightly enriched relative to its abundance in shale rocks (average EF of ~2.2; Table 2), suggesting a dust source could account for at least half of the aerosol Fe budget, while Mn was moderately enriched (average EF of ~ 8; Table 2), indicating an additional, Mn rich source.

Total V concentrations ranged from <0.3 to an upper limit of <11 pmol m^{-3} (Table 2). Only four samples within this range were above the LoD (which varied with sample and analysis run, see Section 2.3), with concentrations ranging from 1.2 to 4.2 pmol m^{-3}. The range of total V concentrations is comparable to observations made several decades or more ago in the Pacific and the north Atlantic (Duce and Hoffman, 1976; Arimoto et al., 1990; Table S3), while considerably higher values have been previously encountered in the western North Atlantic (up to 275 pmol m^{-3}; Duce et al., 1975). Enrichment factors ranged from <1.3 to 28, suggesting a modest contribution to total V from anthropogenic emissions. All V EF values were below the threshold of ~30 (equivalent to a V/Al mass ratio of 0.05) suggested as indicative of a primarily lithogenic source by Sedwick et al., 2007.

Total Co was quantified in ten samples, and upper concentration limits were estimated in a further seven. The range of Co concentrations observed (<0.08 to 4.22 pmol m^{-3}; Table 2) was intermediate between observations made during periods of very low dust deposition (0.09 to 0.19 pmol m^{-3}) and during a Saharan dust event (7 to 18 pmol m^{-3}) in the Sargasso Sea (Shelley et al., 2012). They were also higher than observed at a coastal site in New Zealand (Arimoto et al., 1990; Table S3). Total Zn concentrations (Table 2) were substantially higher than observed in New Zealand (Arimoto et al., 1990; Table S3). As Zn concentrations were high in both total and soluble aerosol measurements (Section 3.3), despite the use of independent analytical techniques, and were also high in rain samples (Section 3.5) which were collected using very different methods, it seems unlikely that the high Zn levels are the result of contamination during sampling or analysis. Total Co and Zn were significantly enriched (average EF of 107 and 241 respectively; Table 2) relative to the elemental ratio in shale, suggesting either a non-crustal source, or a lithogenic source enriched in Zn relative to the shale end-member used here (Co/Al = 0.0001 and Zn/Al = 0.0005; Turekian and Wedepohl, 1961). Patagonian dust, which is assumed to be the primary dust source to the south east Atlantic (Li et al., 2008), can have a molar Co/Al ratio up to ~100 times higher than that of shale (Gaiero et al., 2003; Turekian and Wedepohl., 1961), sufficient to account for the observed Co enrichment. Similarly, molar Zn/Al ratios in Patagonian dust samples were found to range from 0.0006 to 0.0331, with a median 0.0024 (Gaiero et al., 2003). A dust source with a Zn/Al ratio of ~0.03 is sufficient to account for the total Zn enrichment observed here, but a lower ratio would require an additional Zn source to be invoked, which may be anthropogenic, or perhaps from biomass emissions (Nriagu, 1979). Total Zn and Co concentrations were not correlated with each other, implying that they did not have the identical sources, consistent with the above suggestions. These findings highlight the need for improved characterisation of dust sources used as end members in EF calculations.

Total Cu, Ni and Cd concentrations were below the limit of detection of the INAA method for all samples, so are considered only as an estimate of the upper limit on true concentrations. For Cu, Ni and Cd, the substitute values derived from the LoD (see Section 2.3) were higher than typical concentrations observed previously in clean marine aerosol (Volkening & Heumann, 1990; Radlein & Heumann, 1995; Arimoto et al., 1990; Paytan et al., 2009; see Table S3).

3.3. Soluble metal concentrations in aerosol & size distribution

Soluble Fe, Al and Mn concentrations (Table 3) were also comparable to previous observations in remote south Atlantic air (Baker et al., 2013; Gao et al., 2013; see Table S3 in supplementary information), with the majority of values reported here falling at the lower end of these ranges. The two samples with high total Al content (ZD-01 and ZD-02, see section 3.2) also had unusually high soluble Al content and were defined as outliers (Tukey definition). Consistent with earlier work, total and soluble Fe and Al concentrations reported here are among the lowest reported in the Atlantic (e.g. Baker et al., 2013), and are at least an order of magnitude lower than observed in the Saharan outflow (Baker et al., 2013). As for total metal concentrations, there were no systematic trends in the spatial distribution of soluble trace metal concentrations within our data set (Supplementary information, Fig. S2).

In size-segregated samples, the proportion of soluble Fe found in the fine mode (<1 μm diameter) ranged from 24 to 92%, with a median value of 33% (Fig. 4). Similar proportions of soluble Al and Mn were found in the fine mode (Fig. 4), with median values of 36% for Al (range 7 to 79%), and 33% for Mn (range 7 to 64%). These trends are evident in the fully size-segregated samples, in which the highest concentrations of soluble Fe, Al and Mn were found in the 5 to 12 μm diameter fraction (Fig. 5). This distribution is particularly pronounced for Al and Mn, while for Fe the difference in concentrations between the size fractions is less, reflecting a greater contribution of fine material to the total soluble concentration for this element. The largest contributions of the fine mode to the overall soluble Fe content occurred in samples with the highest overall concentrations, and the fine mode dominated soluble Fe concentrations (i.e. >50%) in just four samples (AMT15-27, AMT15-28, AMT15-29 & D357-08). Three of these samples displayed high Fe enrichment factors (EFs of 4.6, 7.7 and 13.3), suggesting an anthropogenic contribution to the fine mode Fe. These results are consistent with a predominantly lithogenic source for Fe, Al and Mn in most samples, with a slightly greater anthropogenic contribution to the Fe loading than for Al or Mn, particularly in samples with a high overall Fe concentration. Baker et al., 2013, also reported wide ranges for the fraction of soluble Fe, Al and Mn found in the fine mode in remote South Atlantic air, though with higher median %fine values (61, 59 and 47% for Fe, Al and Mn respectively). The difference in size-segregation between our results and those of

Baker et al., 2013, likely results from the high levels of variability in trace metal solubility and size distribution, the causes of which are not yet fully understood. Previous studies of the aerosol size distribution in Atlantic remote marine air masses have tended to find the majority of total Fe to reside in the coarse mode: ~64%, ~67% and ~70% of total Fe was found in the coarse mode in samples collected in the south-west Atlantic (Baker et al., 2006a), the tropical Atlantic (Baker et al., 2006b) and the north Atlantic (~17^{o}N; Fomba et al., 2013) respectively. However, ~65% of total Fe was found in the fine mode in a single south Atlantic sample (~11-14^{o}S; Radlein and Heumann, 1995), suggesting variation in the total Fe size distribution can occur. Similarly, the fraction of total Mn in the coarse mode has been reported as ~74% in the south-west Atlantic (Baker et al., 2006a) and ~70% in the tropical Atlantic (Baker et al., 2006b), but only ~50% in remote marine air in the north Atlantic (Fomba et al., 2013). As the size distributions of total metals were not determined in our study, it is not possible to conclude whether the soluble distribution is a function of the total metal distribution, the metal solubility, or both.

Soluble V concentrations were very high during cruise BGH (14 - 463 pmol m^{-3}), and enrichment factors for soluble V relative to total Al ranged from 14 to 2557 indicating a significant non-crustal input. As noted in Section 2.3, we suspect that the BGH samples may have been contaminated by ship stack emissions, as fuel oil is a known source of V (Duce and Hoffman, 1976). (Because total V was not measured during cruise BGH, this issue does not affect our discussion of total V in Section 3.2). This leads to concern that the BGH samples might also be contaminated by other elements for which ship stack emissions are a potential source. However, we do not believe the other elements measured for this cruise (total Fe, Al, Mn and soluble Fe, Al, Mn, Co, Zn, Cu, Cd, Pb) have been affected for the following reasons: (i) Cruises BGH and ZD followed almost identical cruise tracks (Fig. 1), and took place within a few weeks of each other (Table 1), so ambient aerosol trace metal concentrations are likely to be similar. Comparison of the elements measured on both cruises shows V is unique in being anomalously high during BGH (Fig. S2., Supplementary information). This suggests a strong source of V alone during cruise BGH. (ii) Soluble Cu, Cd and Pb were very high during cruise ZD, indicating contamination (Fig S2), but not during BGH; Cu, Cd and Pb concentrations for BGH were not substantially different to those encountered during cruises D357 and JC068. (iii) The high soluble V concentrations encountered during cruise BGH did not correlate with any of the other elements, either total

or soluble, measured in these samples. Excluding samples from cruise BGH, the maximum soluble V concentration was just 3 pmol m^{-3}, and the maximum soluble enrichment factor 26. Of these samples, ~70% had soluble enrichment factors less than 2, indicating that there was not a substantial anthropogenic contribution to the soluble V fraction. The contribution of soluble V to the fine mode could only be quantified in 5 samples, which all had similar values (~82%, Fig. 4). Of these, two samples were substantially enriched in soluble V ($EF \geq 8.5$), consistent with a combustion source, but the remaining three were less enriched ($EF \leq 1.9$). These latter samples suggest a contribution of soluble, lithogenic V to fine mode aerosol in the remote south Atlantic. A similar predominance of total V in the fine aerosol mode (~70%) has been observed in remote north Atlantic air masses (Fomba et al., 2013), suggesting the soluble size distribution we observe reflects the total V distribution.

The majority of soluble Co concentrations (Table 3) were similar to those observed in the Sargasso Sea during a period of low dust loadings (0.05 - 0.18 pmol $m^{-3;}$ Shelley et al., 2012), while the remaining samples had soluble Co concentrations more similar to those observed during a period of high Saharan dust loadings (0.70 - 1.76 pmol $m^{-3;}$ Shelley et al., 2012). Soluble Co was evenly distributed between the coarse and fine modes (Fig. 4).

Soluble Zn concentrations also exhibited a wide range (Table 3), with a small number of high concentration samples (BGH-07, BGH-08, ZD-03, ZD-05). The majority of soluble Zn concentrations were similar to those previously measured in remote south Atlantic air masses using a 0.1M HNO_3 leach (Witt et al., 2006; Table S3). As noted in Section 2.3, soluble Cu and Cd concentrations were anomalously high during cruise ZD (Fig. S4) and so have been excluded from further analysis. Soluble Cu, Ni and Cd concentrations (Table 3) were also in agreement with 0.1M HNO_3 soluble concentrations in remote south Atlantic air masses (Witt et al., 2006; Table S3), while soluble Pb concentrations (Table 3) were lower (Witt et al., 2006; Table S3). The difference in Pb concentrations may reflect the different extraction methods used, although for aerosol from the Indian Ocean, no significant difference in the solubility of Zn, Cu, Ni, Cd was found between the weak acid leach used by Witt et al. (2006) and the pH 4.7 leach employed in this work (Witt et al., 2010). The range of Cu concentrations was very similar to observations made at open ocean locations in the north Atlantic and Pacific (Paytan et al., 2009; Table S3). Assuming the pH4.7 leach extracts

between 35 and 100% of the aerosol Pb (Witt et al., 2010), the soluble Pb concentrations observed here are at the lower end of total Pb concentrations reported for the South Atlantic (Volkening & Heumann,, 1990; Table S3). We speculate this may be attributed to declining levels of atmospheric Pb since the phasing out of Pb as a petrol additive. The percentages of Zn, Cu and Pb found in the fine mode covered a relatively narrow range, at ~72, 55 and 58% respectively (Fig. 4), broadly consistent with anthropogenic high temperature emission sources for these elements. Previous measurements of Atlantic remote marine aerosols have found that total Zn, Cu and Pb are also predominantly found in the fine mode (Radlein & Heumann 1995; Fomba et al., 2013). In contrast, the size distributions of Ni and Cd were extremely variable, with percentages in the fine mode ranging from ~10 to >80% (Fig. 4). Previous studies in similar air masses have found the majority (~70% or more) of total Cd and Ni resides in the fine mode (Radlein & Heumann 1995; Fomba et al., 2013), with this distribution appearing to be ubiquitous for total Cd (Radlein & Heumann 1995). In this case, the variation in soluble size distribution we observe may reflect differences in solubility between the size fractions, rather than variation in total metal loading. As concentrations of total Cu, Ni, Cd and Pb could not be quantified in any samples, we consider the enrichment factors for the soluble fraction of these elements relative to the total Al concentration, which represent a lower limit of EF. All were moderately enriched relative to shale rock abundances, with average EF values of 10 to 174.

3.4. Solubility estimates

The operational definition of solubility used here (see Section 2.2), does not attempt to replicate the dissolution of aerosol particles in seawater, but provides a consistent approach by which the relative solubility of metals in a large sample set can be compared. Fe solubility ranged from 1.3 to 48%, with a median and average of 7 and 11% respectively (Fig. 6). The maximum solubility of 48% occurred for a sample with an unusually high soluble Fe content (BGH-08; 83 pmol m^{-3}), which was identified as an outlier using the Tukey definition. Excluding this point, the range of Fe solubility values (1.3 - 22%) was very similar to that found previously in remote marine aerosol using the same leach protocol (Baker et al., 2006a), and the Southern Ocean using a very similar leach (0.76 to 27%; Gao et al., 2013). These Fe solubilities are higher than found in Saharan dust, but lower than for European air (median values of ~1.7% and ~21% respectively; Baker et al., 2006a). The variation of Fe solubility

with total iron content falls within the envelope of values reported by Sholkovitz et al., 2012 (Fig. 7A), and as such is consistent with an inverse relationship between Fe solubility and total Fe concentration on a global scale. A number of factors have been suggested to contribute to the observed variability in aerosol Fe solubility, including acid processing during atmospheric transport, and mixing of (high solubility) anthropogenic and (low solubility) lithogenic aerosols (Sedwick et al., 2007; Baker and Croot, 2010). Our results do not allow us to identify which of these potential mechanisms dominates over the south-east Atlantic, however low Fe enrichment factors (Section 3.2) and the dominance of the coarse mode soluble Fe (Section 3.3) suggest that the contribution of anthropogenic Fe is less significant than in some other regions, such as the Sargasso Sea, the Bay of Bengal or the East China Sea (Sholkovitz et al., 2012). Fe solubility appears to be slightly higher in samples collected south of 40^{o}S than those collected north of this parallel (Supplementary information, Fig. S3). Average Fe solubility was 20 ± 13% (n=7) in the more southerly samples and 5 ± 3% (n=12) in the northern group; a student's t-test indicated these populations were significantly different (p=2.5%). There are a number of potential causes of this apparent solubility gradient (e.g. higher solubility in more southerly dust sources, longer periods of atmospheric processing in the more southerly samples, differences in aerosol pH due to latitudinal variation in gaseous emissions), and we are not able to identify which of these processes is responsible here. It is also possible that systematic biases, for example seasonality in aerosol sources, transport and/or processing, may have caused this apparent spatial divide, as all southerly samples were collected during the Z-D and BGH cruises. Recent work in the Pacific has found that aerosol Fe solubility does not increase with distance from source (Buck et al., 2013); further work is needed to improve understanding of spatial variation in trace metal solubility.

Al solubility ranged from 3 to 78%, with a median of 16% (Fig. 6). As for Fe, the median aerosol Al solubility is similar to that previously reported for the same air mass type (~18%, Baker et al., 2006a). However, Al solubilities here are higher than reported for both Saharan dust and European air masses (Baker et al., 2006a). A very wide range of Mn solubilities was also encountered (1 to 82%) in common with Baker et al., 2006a, who report a solubility range of 18 - 75% in south Atlantic Remote aerosol. Mn solubility was inversely associated with Total Mn content, exhibiting an approximately hyperbolic relationship (R^2 = 0.54 for correlation between the natural log of the two variables), similar in appearance to that

observed between iron solubility and total iron loadings (Sedwick et al., 2007; Sholkovitz et al., 2012). However, unlike Fe, this distribution is not observed for Mn on a larger scale (Fig. 7b; Baker et al., 2014). In our dataset, the distribution could be considered to arise from a cluster of higher concentration samples (≥ 18.5 pmol m^{-3}) all having solubility below ~12%, and a cluster of lower concentration samples (≤ 10.1 pmol m^{-3}) with solubility ranging from ~12 to 82% (Fig. 7B). The solubilities of the former cluster are much lower than observed in other Atlantic air mass types, both lithogenic and anthropogenic, using the same leach protocol (e.g. Saharan air ~55%, European air ~45%; Baker et al, 2006a; see Fig. 7B). Mn solubility and Mn enrichment factor also displayed an apparently hyperbolic relationship, with a correlation between the natural log of the two variables of $R^2 = 0.65$. The high concentration, low solubility samples had an average EF of 21 ± 15 (median 18) while the lower concentration, higher solubility samples had an average EF of 2 ± 1 (median 2). It is not clear what has caused this cluster of samples with very low Mn solubility and high enrichment factors. They tended to occur to the east of the sampling region (Supplementary information, Figs S1, S2 and S3), and most, but not all, were collected during cruise D357. Patagonian dust has an Mn/Al molar ratio (0.0035 - 0.0055; Gaiero et al., 2003) similar to that of Shale (0.0052; Turekian and Wedepohl, 1961), so regional differences in the crustal ratio are not likely to be the cause of the enrichment. Desert varnishes may become separated from their parent surfaces via abrasion during saltation (Bullard et al., 2004; Mackie et al., 2006), Such varnishes have been reported to have extremely high Mn/Al ratios (>1 mol mol^{-1}), with the Mn predominantly found as insoluble Mn(IV) (Potter and Rossman, 1979). However, we are not able to confirm the presence of desert varnish fragments in our samples. Industrial processes (e.g. steel production, fossil fuel combustion) can also release Mn to the atmosphere.

As a large number of the V samples were below the limit of detection, it was only possible to quantify solubility for three samples. This yielded values of 16, 67 and 92%. A wide range of solubilities have previously been reported for marine aerosol (e.g. of ~5-7% in Saharan aerosol and ~40-90% in aerosol assumed to be anthropogenic; Sholkovitz et al., 2009). Average cobalt solubility for the SE Atlantic aerosol samples was 2 ± 1% (Fig. 6), which is in contrast to earlier work, which reports 75-100% solubility (using deionised water leaches) for marine aerosols of a predominantly North American origin, and 8-10% for aerosol with higher mineral dust content (Shelley et al., 2012). The low Co solubility of the south-east

Atlantic aerosols is more similar to that observed for fine (<20 μm) coal ash dust (0.73%) and loess soil (0.145%) in seawater (Thuróczy et al., 2010). Such a wide range of potential solubility means that the impact of atmospheric Co deposition on the dissolved Co budget is likely to be highly dependent on the nature of the aerosol, as well as the Co loading. As with Mn, Co solubility was inversely related to total Co loading and enrichment factor. If the Co enrichment is due to an anthropogenic contribution, this contradicts the general paradigm that trace metals in anthropogenic material are more soluble than those in lithogenic material. Alternatively, the enrichment in low solubility Co may be explained by a lithogenic source with an elevated Co/Al ratio relative to shale, such as Patagonian dust (see Section 3.2). In contrast, Zn solubility ranged from 66 to 97% (Table 3). Similarly high Zn solubilities have previously been observed using the same pH4.7 leach in aerosols from the Indian Ocean (Witt et al., 2010), and also for anthropogenic Zn in rainwater with a pH below 5 (Lim et al., 1994). The values are strikingly different to the solubility in seawater of Zn from both coal ash dust (5%) and loess soil (16%; Thuróczy et al., 2010), presumably due to the differing pH of the dissolution matrix. The high solubility, high enrichment factors and high percentage in the fine mode for Zn are consistent with an anthropogenic source for this element.

3.5. Dry deposition flux estimates (total and soluble metals)

The choice of deposition velocity introduces a high level of uncertainty into the calculation of dry aerosol deposition (Duce et al., 1991; Schulz et al., 2012). Although wind speed and particle size dependent parameterisations for V_d are available (e.g. Ganzeveld et al., 1998), values generated are still subject to large uncertainties, particularly when aerosol size distribution is not well known, and the use of single values of V_d to estimate deposition fluxes from aerosol concentrations is still standard. Reflecting the suggested two- to three-fold uncertainty in V_d (Duce et al., 1991), we have estimated dry deposition fluxes using two different V_d values appropriate to different aerosol size classes (Table 4). Uncertainties in V_d remain one of the largest contributors to uncertainty in estimates of dry deposition (Schulz et al., 2012); in order to resolve this, alternative approaches such as the estimation of dust deposition from the water column Al concentrations, as in the MADCOW model (Measures and Vink, 2000), or Th isotope budgets (Hsieh et al., 2011) are clearly also required.

Consistent with the similar atmospheric concentrations employed, and the dominance of remote marine air masses in the study region, our estimates of total and soluble deposition

fluxes of Fe, Al and Mn (Table 3) were broadly similar to climatological estimates of deposition for the south east Atlantic (Baker et al., 2013). In general, median deposition fluxes for our sample set were lower than the climatological values using the lower V_d value of 0.3 cm s^{-1}, but very similar when the higher value of 1 cm s^{-1} was applied. In either case, the range of our observations encompassed the climatological value. Despite the use of an even higher value of V_d (1.3 cm s^{-1}) than here, Heimburger et al., 2012 estimated lower total Al deposition fluxes for Kerguelen Island, reflecting the lower atmospheric concentrations (see section 3.2). To the best of our knowledge, V dry deposition has not previously been estimated for the south Atlantic. Duce and Hoffman, 1976, used a V_d value of 0.38 cm s^{-1} to estimate a total V dry deposition flux to the ocean between 30 and 60^{o}N of 0.8 nmol m^{-2} d^{-1}. This value is similar to that reported here (Table 4), reflecting the similar aerosol V concentrations observed (Section 3.2). Where the same value of V_d is used (1 cm s^{-1}), median values of total and soluble Co deposition fluxes were comparable to those observed in the Sargasso Sea during a period of low aerosol trace metal loadings (0.08 - 0.16 nmol m^{-2} d^{-1} total Co, 0.047 - 0.155 nmol m^{-2} d^{-1} soluble Co; Shelley et al., 2012), though the range of values was somewhat larger (Table 4). Estimates of soluble Pb dry deposition were ~30% of the estimated total dry Pb flux to the South Atlantic (Duce et al., 1991), consistent with the observed range of Pb dissolution using the pH4.7 leach (32 to 100%; Witt et al., 2010), and possibly also reflecting declining atmospheric Pb levels since 1991.

3.6. Wet deposition flux estimates

The concentrations of Fe, Al and Mn in the rainwater samples we collected (Table 5) were approximately an order of magnitude higher than observed previously in the south-east Atlantic (Kim and Church, 2002; Baker et al., 2013), and the south-west Atlantic (Helmers and Schrems, 1995). Pb, Zn and Cu were also an order of magnitude higher than previously observed in the south Atlantic (Helmers and Schrems, 1995). The ship was facing into the wind during all rain sampling (i.e. the conditions for clean aerosol sampling were satisfied), so contamination from the ship itself is thought to have been minimal. Although three of the six rain samples were collected very close to South Africa, back trajectories indicated that the air masses were all of marine origin. In one sample (D357-R05) the marine air had circled over the South African coast before arriving at the sampling location, but trace metal concentrations in this sample fell within the ranges of the other samples, suggesting contact

with the coast was not responsible for elevated concentrations. We therefore consider that the high concentrations we observed probably reflect the extremely low volumes of rain collected, as a result of only brief, light rain events being encountered during the cruises. Concentrations of rainwater constituents are generally inversely related to rainfall amount, due to the so-called 'wash-out' effect at the onset of rain events (Helmers and Schrems, 1995). While our sample volumes were extremely small (10 to 50 mL; see Table S1, Supplementary information), previous observations in the south Atlantic have generally been based on higher-volume samples (1900 - 2000 mL - Kim and Church, 2002; 30 - 227 mL - Baker et al., 2013; 30 - 100 mL - Helmers and Schrems, 1995). In contrast, comparable V, Co, Cu, Cd and Pb concentrations have been reported for small volume samples (20 - 30 mL) collected in the Indian Ocean (Witt et al., 2010).

Meanwhile, Co, Cd and Ni were around an order of magnitude lower than observed previously in higher volume samples from the south Atlantic (Helmers and Schrems, 1995). As these samples were all collected to the west and/or north of our study region, we tentatively suggest these differences may reflect gradients in atmospheric concentrations across the Atlantic that are sufficiently large as to not be removed by the sample volume effect. Specifically, atmospheric concentrations of Co, Cd, and Ni may be lower in our more remote sampling region. Similarly, Ni concentrations were substantially lower than reported for similar volume samples from the Indian Ocean (Witt et al., 2010).

The sampling and analysis protocol used for wet deposition yields a measure of total metal concentration, although note this is not an identical operational definition to 'total' with regard to the aerosol samples. 'Soluble' metal concentrations in wet deposition were not measured. A compilation of data presented in Baker et al., 2013, gives median solubility (based on the same operational definition as here) in Atlantic wet deposition as ~9, 12 and 74% for Fe, Al and Mn respectively. Pb, Zn and Cu solubility in marine rainwater varies from ~10-20 to ~80-90%, with a strong dependence on pH over a narrow limiting band (Spokes and Jickells, 1995; Chester et al., 2000).

Wet deposition estimates based on small numbers of samples are subject to large uncertainty, especially when, as here, the rain samples were collected non-uniformly across the study region and may not represent the full range of precipitation conditions (Fig. 2). The uncertainties associated with both the volume weighted mean rainwater concentrations (40 - 114% RSD), and the areal weighted mean precipitation rate (64% RSD) were both high, leading to estimated uncertainties on the wet deposition fluxes of ~100% RSD. The results for V, Ni, Cu and Cd should be treated with particular caution, as the majority of samples were below the limit of detection for these elements (Table 5). Given these uncertainties, the total wet deposition fluxes for Fe, Al and Mn we have estimated (Table 5) are broadly similar to those previously estimated for the South Atlantic (Baker et al., 2013). Values are one to two orders of magnitude greater than previously reported for the low-precipitation eastern South Atlantic, but similar to the equivalent values for the high-precipitation western South Atlantic (Baker et al., 2013). This result is probably partly due to differences in regional precipitation rates: the climatological average precipitation rate for our study region over the months October to January (areal weighted mean precipitation rate of 1.43 ± 0.9 mm day^{-1}; Xie and Arkin, 1997) was higher than the seasonal average values (0.6 – 1.0 mm day^{-1} for Region 4 of Baker et al. (2013). As discussed previously (Baker et al., 2010; Baker et al., 2013), small sample numbers and sizes, and non-representative sample distribution further contribute to uncertainty in wet deposition flux estimates and likely account for these differences. Nevertheless, the wet deposition Al flux is similar to that reported for a much more comprehensive precipitation record at Kerguelen (Heimburger et al., 2012). Co wet deposition was higher than estimated for the Sargasso Sea (soluble Co: 190-620 pmol m^{-2} day^{-1} ; Shelley et al., 2012).

For most elements, wet deposition flux estimates were far greater than dry deposition flux estimates (Tables 4 and 5). A substantial contribution from wet deposition is consistent with model results, which found wet deposition to account for 80% of Patagonian dust deposition to the open ocean (Johnson et al., 2010). Dust deposition has also been found to be controlled by wet deposition over the Kerguelen Islands (Heimburger et al., 2012). Our results suggest wet deposition of total Co could account for most of the total cobalt deposition flux (77 to 96%), which is similar to the estimate of >80% made for Bermuda (see Shelley et al., 2012). Similarly, the very high contribution of wet deposition to our estimated total Pb flux (92-99%) is broadly consistent with the findings of Duce et al., who estimated that globally 83% of Pb

deposition to the oceans is wet (Duce et al., 1991). However, as already discussed, both wet and dry deposition fluxes are subject to large uncertainties. Due to the large uncertainty associated with the wet deposition flux estimates (Table 5), it is not possible to conclude definitively that wet deposition is the dominant term. It is also possible that our wet deposition fluxes are over-estimates resulting from particularly low rainfall rates, and hence high rainwater concentrations, encountered during the cruises (see above). As the wet deposition fluxes are so much greater than the dry deposition fluxes, the uncertainty in the latter does not substantially alter the outcome of this analysis. For example, even using the higher V_d value of 1 cm s^{-1}, wet deposition still accounted for ~80 to ~90% of the total deposition of Fe, Al, Mn and Co. However, Nevertheless, despite the uncertainties in our deposition flux estimates, the contribution of the dry deposition term to the total deposition tends to be comparable to the lower limit of the wet deposition flux, and even a cautious interpretation of these results points to a significant contribution from wet deposition in the south-east Atlantic region. Further research is required to better constrain wet deposition fluxes in remote marine areas.

Total (wet plus dry) deposition fluxes were comparable to previous estimates for the South Atlantic and South Indian Ocean for Fe, Al, Mn, Cd and Ni, but were an order of magnitude higher for V, Co and Cu and two orders of magnitude higher for Zn and Pb (Duce et al., 1991; Heimburger et al., 2013; Baker et al., 2013). The discrepancies for the latter elements are driven by the high wet deposition flux term here. Note in the case of V and Cu, the wet deposition fluxes are upper limits due to most of the samples being below the LoD (Table 5), and so the true values may in fact be closer to the literature values. Assuming that mineral dust is 8% Al by mass (Turekian and Wedepohl., 1961), a total dust deposition flux of 412 μg m^{-2} d^{-1} is obtained, in broad agreement with recent models (Johnson et al., 2010).

Wet deposition fluxes were also estimated from the aerosol total metal concentrations and the scavenging ratio (S_R), using equation 5 below:

$$F_{wet} = P \bullet C_{atm} \bullet S_R / \rho \qquad (5)$$

The density of air (ρ) was 1200 g m^{-3}. A value of 200 was used for S_R (Duce et al., 1991). The wet deposition fluxes obtained in this manner were all one to two orders of magnitude

lower than the fluxes calculated from direct measurements of rainfall concentrations, and fell very close to or just outside the estimated uncertainty (Table 5). This may suggest the value of 200 for S_R is too low in this case, consistent with S_R being subject to high uncertainty (Duce et al., 1991). The results may imply that the cloud (and subsequently, rainwater) droplets were formed under conditions of higher aerosol trace metal concentrations, and that the trace metals accumulated within them are not solely a function of aerosol concentrations within the sampling region. Similarly, Heimburger et al. (2012) calculated very large wet scavenging ratios (>>200) from observed concentrations of Al, Na and Mg in wet and dry deposition collected on the Kerguelen Islands. Our results support their conclusion that the calculation of total deposition fluxes from surface aerosol concentrations alone is not appropriate at remote marine locations where surface aerosol concentrations may not represent the total air column over which scavenging by wet deposition occurs.

4. Conclusions

Aerosol and rain trace metal concentrations have been measured in remote marine air masses over the south-east Atlantic Ocean. Total and soluble Fe, Al, Mn and V concentrations were typically similar to those reported previously for comparable air mass types, being low compared to measurements made in the Saharan dust outflow and polluted northern hemisphere (Section 3.2 and 3.3). A greater proportion of soluble Fe, Al and Mn was found in the coarse mode than the fine mode (Fig. 3), and these were only moderately enriched relative to crustal material (Table 2), suggesting a predominantly lithogenic source for these elements. Meanwhile total Co and Zn were significantly enriched (Table 2), possibly because the Patagonian dust has higher Co/Al, and perhaps also Zn/Al ratios, than the shale end member end member used to calculate enrichment factors. Soluble Cu, Ni, Cd and Pb concentrations were consistent with previous measurements, and indicated moderate levels of enrichment relative to crustal material (Section 3.3). Fe solubility ranged from 1.3 to 22%, in agreement with previous measurements in the region (Fig. 4). A very wide range of solubilities were observed for Al, Mn and V, while Co and Zn solubilities were relatively well constrained at ~2 and 66-97% respectively (Fig. 4). These results highlight the large uncertainties still associated with trace metal solubility in atmospheric deposition.

Wet deposition massively dominated our estimates of total (wet plus dry) deposition fluxes for all elements except Ni (Section 3.6). However, our estimates of wet deposition are subject to high levels of uncertainty, due to the small number of samples, their low volume and low elemental concentrations (relative to our limits of detection), and inhomogeneity in both rainwater concentrations and precipitation rates across the study region. Given there appears to be a substantial contribution of wet deposition to total deposition fluxes, there is a need for wet deposition fluxes to be better constrained. As it may not be appropriate to calculate wet deposition in remote marine locations using scavenging ratios (Heimburger et al., 2012; section 3.6), we suggest this will require a much larger database of rainwater observations.

Acknowledgements

We thank M. Waeles, S. Ussher, T. Lesworth, R. Middag and E. Verdeny for collecting samples during the AMT15, AMT16, AMT17, ZD and BGH cruises. This work was carried out with funding from the UK Natural Environment Research Council (NERC) under grants NE/E010180/1 and NE/H00548X/1. We gratefully acknowledge the NOAA Air Resources Laboratory for the provision of the HYSPLIT transport and dispersion model and READY website (http://www.arl.noaa.gov/HYSPLIT.php). We also thank the anonymous reviewers, whose suggestions have improved the manuscript.

References

Arimoto, R., B. J. Ray, R. A. Duce, A. D. Hewitt, R. Boldi, and A. Hudson (1990), Concentrations, sources, and fluxes of trace-elements in the remote marine atmosphere of New Zealand, J. Geophys. Res.: Atmos., 95(D13), 22389-22405, doi:10.1029/JD095iD13p22389.

Baker, A. R., C. Adams, T. G. Bell, T. D. Jickells, and L. Ganzeveld (2013), Estimation of atmospheric nutrient inputs to the Atlantic Ocean from 50 degrees N to 50 degrees S based on large-scale field sampling: Iron and other dust-associated elements, Glob. Biogeochem. Cycles, 27(3), 755-767, doi:10.1002/gbc.20062.

Baker, A. R., and P. L. Croot (2010), Atmospheric and marine controls on aerosol iron solubility in seawater, Mar. Chem., 120(1-4), 4-13, doi:10.1016/j.marchem.2008.09.003.

Baker, A. R., T. D. Jickells, M. Witt, and K. L. Linge (2006a), Trends in the solubility of iron, aluminium, manganese and phosphorus in aerosol collected over the Atlantic Ocean, Mar. Chem., 98(1), 43-58, doi:10.1016/j.marchem.2005.06.004.

Baker, A. R., M. French, and K. L. Linge (2006b), Trends in aerosol nutrient solubility along a west-east transect of the Saharan dust plume, Geophys. Res. Lett., 33(7), 4, doi:10.1029/2005gl024764.

Baker, A. R., O. Laskina, and V. H. Grassian (2014), Processing and Ageing in the Atmosphere, in Mineral Dust: A key player in the Earth System, edited by P. Knippertz and J. Stuut, -B.W., Springer.

Baker, A. R., T. Lesworth, C. Adams, T. D. Jickells, and L. Ganzeveld (2010), Estimation of atmospheric nutrient inputs to the Atlantic Ocean from 50 degrees N to 50 degrees S based on large-scale field sampling: Fixed nitrogen and dry deposition of phosphorus, Glob. Biogeochem. Cycles, 24, doi:10.1029/2009gb003634.

Baker, A. R., K. Weston, S. D. Kelly, M. Voss, P. Streu, and J. N. Cape (2007), Dry and wet deposition of nutrients from the tropical Atlantic atmosphere: Links to primary productivity and nitrogen fixation, Deep-Sea Research Part I-Oceanographic Research Papers, 54(10), 1704-1720, doi:10.1016/j.dsr.2007.07.001.

Barry, R. G., and R. J. Chorley (1971), Atmosphere, weather and climate, 2nd Ed., Methuen, London, UK.

Bown, J., M. Boye, A. Baker, E. Duvieilbourg, F. Lacan, F. Le Moigne, F. Planchon, S. Speich, and D. M. Nelson (2011), The biogeochemical cycle of dissolved cobalt in the Atlantic and the Southern Ocean south off the coast of South Africa, Mar. Chem., 126(1-4), 193-206, doi:10.1016/j.marchem.2011.03.008.

Boye, M., B. D. Wake, P. L. Garcia, J. Bown, A. R. Baker, and E. P. Achterberg (2012), Distributions of dissolved trace metals (Cd, Cu, Mn, Pb, Ag) in the southeastern Atlantic and the Southern Ocean, Biogeosciences, 9(8), 3231-3246, doi:10.5194/bg-9-3231-2012.

Buck, C. S., W. M. Landing, and J. Resing (2013), Pacific Ocean aerosols: Deposition and solubility of iron, aluminum, and other trace elements, Mar. Chem., 157, 117-130, doi:10.1016/j.marchem.2013.09.005.

Bullard, J. E., G. H. McTainsh, and C. Pudmenzky (2004), Aeolian abrasion and modes of fine particle production from natural red dune sands: an experimental study, Sedimentology, 51(5), 1103-1125, doi:10.1111/j.1365-3091.2004.00662.x.

Cassar, N., M. L. Bender, B. A. Barnett, S. Fan, W. J. Moxim, H. Levy, II, and B. Tilbrook (2007), The Southern Ocean biological response to Aeolian iron deposition, Science, 317(5841), 1067-1070, doi:10.1126/science.1144602.

Chester, R., M. Nimmo, G. R. Fones, S. Keyse, and J. Zhang (2000), The solubility of Pb in coastal marine rainwaters: pH-dependent relationships, Atmos. Environ., 34(23), 3875-3887, doi:10.1016/s1352-2310(00)00177-1.

Dixon, J. L. (2008), Macro and micro nutrient limitation of microbial productivity in oligotrophic subtropical Atlantic waters, Environmental Chemistry, 5(2), 135-142, doi:10.1071/en07081.

Draxler, R. R., and G. D. Rolph HYSPLIT (HYbrid Single-Particle Lagrangian Integrated Trajectory) Model access via NOAA ARL READY Website (http://www.arl.noaa.gov/HYSPLIT.php). NOAA Air Resources Laboratory, College Park, MD., edited.

Duce, R. A., and G. L. Hoffman (1976), Atmospheric vanadium transport to ocean, Atmos. Environ., 10(11), 989-996, doi:10.1016/0004-6981(76)90207-9.

Duce, R. A., G. L. Hoffman, and W. H. Zoller (1975), Atmospheric trace-metals at remote northern and southern-hemisphere sites - Pollution or Natural, Science, 187(4171), 59-61, doi:10.1126/science.187.4171.59.

Duce, R. A., P. S. Liss, J. T. Merrill, E. L. Atlas, P. Buat-Menard, B. B. Hicks, J. M. Miller, J. M. Prospero, R. Arimoto, and et al. (1991), The atmospheric input of trace species to the world ocean, Glob. Biogeochem. Cycles, 5(3), 193-260, doi:10.1029/91gb01778.

Fomba, K. W., K. Muller, D. van Pinxteren, and H. Herrmann (2013), Aerosol size-resolved trace metal composition in remote northern tropical Atlantic marine environment: case study Cape Verde islands, Atmos. Chem. Phys., 13(9), 4801-4814, doi:10.5194/acp-13-4801-2013.

Gaiero, D. M., J. L. Probst, P. J. Depetris, S. M. Bidart, and L. Leleyter (2003), Iron and other transition metals in Patagonian riverborne and windborne materials: Geochemical

control and transport to the southern South Atlantic Ocean, Geochim. Cosmochim. Acta, 67(19), 3603-3623, doi:10.1016/s0016-7037(03)00211-4.

Gaiero, D. M., P. J. Depetris, J. L. Probst, S. M. Bidart, and L. Leleyter (2004), The signature of river- and wind-borne materials exported from Patagonia to the southern latitudes: a view from REEs and implications for paleoclimatic interpretations, Earth Planet. Sci. Lett., 219(3-4), 357-376, doi:10.1016/s0012-821x(03)00686-1.

Gao, Y., G. Xu, J. Zhan, J. Zhang, W. Li, Q. Lin, L. Chen, and H. Lin (2013), Spatial and particle size distributions of atmospheric dissolvable iron in aerosols and its input to the Southern Ocean and coastal East Antarctica, J. Geophys. Res.: Atmos., 118(22), 12634-12648, doi:10.1002/2013jd020367.

Ganzeveld, L., J. Lelieveld, and G. J. Roelofs (1998), A dry deposition parameterization for sulfur oxides in a chemistry and general circulation model, J. Geophys. Res.: Atmos., 103(D5), 5679-5694, doi:10.1029/97jd03077.

Guieu, C., R. Duce, and R. Arimoto (1994), Dissolved input of manganese to the ocean - aerosol source, J. Geophys. Res.: Atmos., 99(D9), 18789-18800, doi:10.1029/94jd01120.

Heimburger, A., R. Losno, S. Triquet, F. Dulac, and N. Mahowald (2012), Direct measurements of atmospheric iron, cobalt, and aluminum-derived dust deposition at Kerguelen Islands, Glob. Biogeochem. Cycles, 26, doi:10.1029/2012gb004301.

Heimburger, A., R. Losno, S. Triquet, and E. B. Nguyen (2013), Atmospheric deposition fluxes of 26 elements over the Southern Indian Ocean: Time series on Kerguelen and Crozet Islands, Glob. Biogeochem. Cycles, 27(2), 440-449, doi:10.1002/gbc.20043.

Helmers, E., and O. Schrems (1995), Wet deposition of metals to the tropical North and the South Atlantic Ocean, Atmos. Environ., 29(18), 2474-2484.

Hsieh, Y. T., G. M. Henderson, and A. L. Thomas (2011), Combining seawater Th-232 and Th-230 concentrations to determine dust fluxes to the surface ocean, Earth Planet. Sci. Lett., 312(3-4), 280-290, doi:10.1016/j.epsl.2011.10.022.

Jickells, T. D., et al. (2005), Global iron connections between desert dust, ocean biogeochemistry, and climate, Science, 308(5718), 67-71, doi:10.1126/science.1105959.

Johnson, M. S., N. Meskhidze, F. Solmon, S. Gasso, P. Y. Chuang, D. M. Gaiero, R. M. Yantosca, S. L. Wu, Y. X. Wang, and C. Carouge (2010), Modeling dust and soluble iron deposition to the South Atlantic Ocean, J. Geophys. Res.: Atmos., 115, doi:10.1029/2009jd013311.

Jordi, A., G. Basterretxea, A. Tovar-Sanchez, A. Alastuey, and X. Querol (2012), Copper aerosols inhibit phytoplankton growth in the Mediterranean Sea, Proc. Natl. Acad. Sci. U.S.A., 109(52), 21246-21249, doi:10.1073/pnas.1207567110.

Kim, G., and T. M. Church (2002), Wet deposition of trace elements and radon daughter systematics in the South and equatorial Atlantic atmosphere, Glob. Biogeochem. Cycles, 16(3), doi:10.1029/2001gb001407.

Li, F., P. Ginoux and V. Ramaswamy. (2008). Distribution, transport and deposition of mineral dust in the Southern Ocean and Antarctica: Contribution of major sources. J. Geophys. Res.: Atmos., 113, doi:10.1029/2007/JD009190.

Lim, B., T. D. Jickells, J. L. Colin, and R. Losno (1994), Solubilities of Al, Pb, Cu, and Zn in rain sampled in the marine environment over the North Atlantic ocean and Mediterranean Sea, Glob. Biogeochem. Cycles, 8(3), 349-362, doi:10.1029/94gb01267.

Losno, R., G. Bergametti, and P. Carlier (1992), Origins of atmospheric particulate matter over the North Sea and the Atlantic Ocean, J. Atmos. Chem., 15(3-4), 333-352, doi:10.1007/bf00115403.

Mackie, D. S., J. M. Peat, G. H. McTainsh, P. W. Boyd, and K. A. Hunter (2006), Soil abrasion and eolian dust production: Implications for iron partitioning and solubility, Geochemistry Geophysics Geosystems, 7, 11, doi:10.1029/2006gc001404.

Measures, C. I., and S. Vink (2000), On the use of dissolved aluminum in surface waters to estimate dust deposition to the ocean, Glob. Biogeochem. Cycles, 14(1), 317-327, doi:10.1029/1999gb001188.

Moore, C. M., et al. (2009), Large-scale distribution of Atlantic nitrogen fixation controlled by iron availability, Nat. Geosci., 2(12), 867-871, doi:10.1038/ngeo667.

Moore, C. M., et al. (2013), Processes and patterns of oceanic nutrient limitation, Nat. Geosci., 6(9), 701-710, doi:10.1038/ngeo1765.

Morton, P. L., et al. (2013), Methods for the sampling and analysis of marine aerosols: results from the 2008 GEOTRACES aerosol intercalibration experiment, Limnology and Oceanography-Methods, 11, 62-78, doi:10.4319/lom.2013.11.62.

Nriagu, J. O. (1979), Global inventory of natural and anthropogenic emissions of trace metals to the atmosphere, Nature, 279(5712), 409-411, doi:10.1038/279409a0.

Panzeca, C., A. J. Beck, K. Leblanc, G. T. Taylor, D. A. Hutchins, and S. A. Sanudo-Wilhelmy (2008), Potential cobalt limitation of vitamin B(12) synthesis in the North Atlantic Ocean, Glob. Biogeochem. Cycles, 22(2), 7, doi:10.1029/2007gb003124.

Paytan, A., K. R. M. Mackey, Y. Chen, I. D. Lima, S. C. Doney, N. Mahowald, R. Labiosa, and A. F. Postf (2009), Toxicity of atmospheric aerosols on marine phytoplankton, Proc. Natl. Acad. Sci. U.S.A., 106(12), 4601-4605, doi:10.1073/pnas.0811486106.

Potter, R. M., and G. R. Rossman (1979), Manganese oxide and iron oxide mineralogy of desert varnish, Chemical Geology, 25(1-2), 79-94, doi:10.1016/0009-2541(79)90085-8.

Radlein, N., and K. G. Heumann (1992), Trace analysis of heavy metals in aerosols over the Atlantic Ocean from Antarctica to Europe, International Journal of Environmental Analytical Chemistry, 48(2), 127-150, doi:10.1080/03067319208027046.

Radlein, N., and K. G. Heumann (1995), Size fractionated impactor sampling of aerosol particles over the Atlantic Ocean from Europe to Antarctica as a methodology for source identification of Cd, Pb, Tl, Ni, Cr, and Fe, Fresenius Journal of Analytical Chemistry, 352(7-8), 748-755, doi:10.1007/bf00323059.

Saito, M. A., and T. J. Goepfert (2008), Zinc-cobalt colimitation of Phaeocystis antarctica, Limnol. Oceanogr., 53(1), 266-275, doi:10.4319/lo.2008.53.1.0266.

Sarthou, G., et al. (2003), Atmospheric iron deposition and sea-surface dissolved iron concentrations in the eastern Atlantic Ocean, Deep-Sea Research Part I-Oceanographic Research Papers, 50(10-11), 1339-1352, doi:10.1016/s0967-0637(03)00126-2.

Schlitzer, R. (2014), Ocean Data View, edited, http://odv.awi.de.

Schulz, M., et al. (2012), Atmospheric Transport and Deposition of Mineral Dust to the Ocean: Implications for Research Needs, Environ. Sci. Technol., 46(19), 10390-10404, doi:10.1021/es300073u.

Sedwick, P. N., E. R. Sholkovitz, and T. M. Church (2007), Impact of anthropogenic combustion emissions on the fractional solubility of aerosol iron: Evidence from the Sargasso Sea, Geochemistry Geophysics Geosystems, 8, doi:10.1029/2007gc001586.

Shelley, R. U., et al. (2012), Controls on dissolved cobalt in surface waters of the Sargasso Sea: Comparisons with iron and aluminum, Glob. Biogeochem. Cycles, 26, doi:10.1029/2011gb004155.

Sholkovitz, E. R., P. N. Sedwick, and T. M. Church (2009), Influence of anthropogenic combustion emissions on the deposition of soluble aerosol iron to the ocean: Empirical estimates for island sites in the North Atlantic, Geochim. Cosmochim. Acta, 73(14), 3981-4003, doi:10.1016/j.gca.2009.04.029.

Sholkovitz, E. R., P. N. Sedwick, T. M. Church, A. R. Baker, and C. F. Powell (2012), Fractional solubility of aerosol iron: Synthesis of a global-scale data set, Geochim. Cosmochim. Acta, 89, 173-189, doi:10.1016/j.gca.2012.04.022.

Slinn, S. A., and W. G. N. Slinn (1980), Predictions for particle deposition on natural waters, Atmos. Environ., 14(9), 1013-1016, doi:10.1016/0004-6981(80)90032-3.

Spokes, L. J., and T. D. Jickells (1995), Speciation of metals in the atmosphere, 137-168 pp.

Thuroczy, C. E., M. Boye, and R. Losno (2010), Dissolution of cobalt and zinc from natural and anthropogenic dusts in seawater, Biogeosciences, 7(6), 1927-1936, doi:10.5194/bg-7-1927-2010.

Turekian, K. K., and K. H. Wedepohl (1961), Distribution of the elements in some major units of the Earth's crust, Geological Society of America Bulletin, 72(2), 175-191.

Ussher, S. J., E. P. Achterberg, C. Powell, A. R. Baker, T. D. Jickells, R. Torres, and P. J. Worsfold (2013), Impact of atmospheric deposition on the contrasting iron biogeochemistry of the North and South Atlantic Ocean, Glob. Biogeochem. Cycles, 27(4), 1096-1107, doi:10.1002/gbc.20056.

Volkening, J., and K. G. Heumann (1990), Heavy metals in the near surface aerosol over the Atlantic Ocean from 60 degrees South to 54 degrees North, J. Geophys. Res.: Atmos., 95(D12), 20623-20632, doi:10.1029/JD095iD12p20623.

Witt, M., A. R. Baker, and T. D. Jickells (2006), Atmospheric trace metals over the Atlantic and South Indian Oceans: Investigation of metal concentrations and lead isotope ratios in coastal and remote marine aerosols, Atmos. Environ., 40(28), 5435-5451, doi:10.1016/j.atmosenv.2006.04.041.

Witt, M. L. I., T. A. Mather, A. R. Baker, J. C. M. De Hoog, and D. M. Pyle (2010), Atmospheric trace metals over the south-west Indian Ocean: Total gaseous mercury, aerosol trace metal concentrations and lead isotope ratios, Mar. Chem., 121(1-4), 2-16, doi:10.1016/j.marchem.2010.02.005.

Xie, P. P., and P. A. Arkin (1997), Global precipitation: A 17-year monthly analysis based on gauge observations, satellite estimates, and numerical model outputs, Bulletin of the American Meteorological Society, 78(11), 2539-2558.

Figures

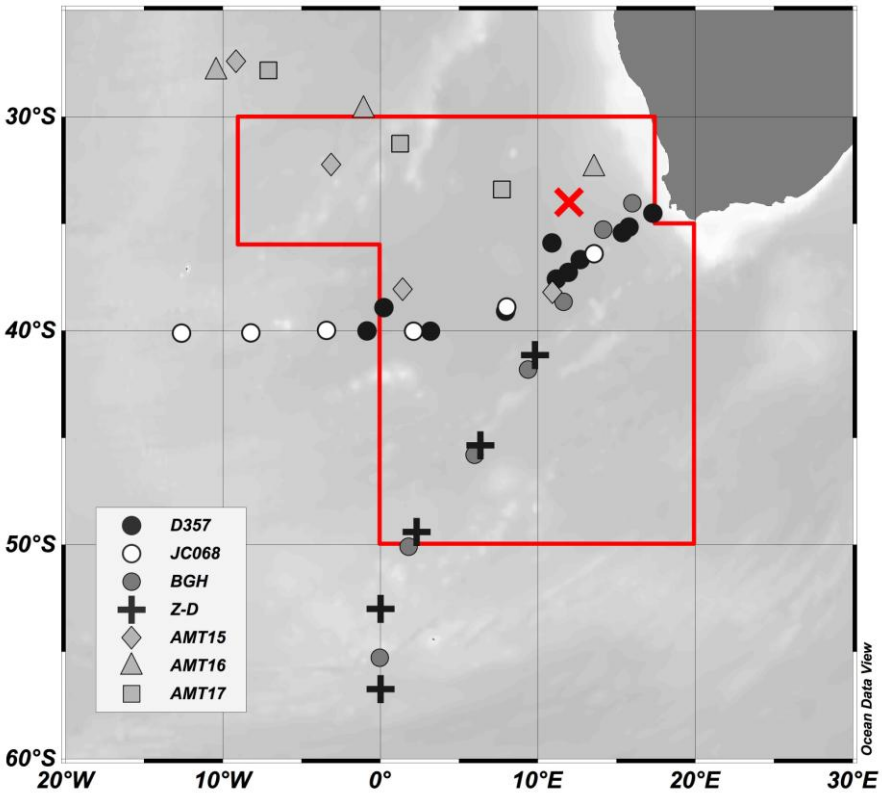

Fig. 1. Aerosol sample mid-points (grey symbols). Region 4d and arrival point of back trajectories used to produce air mass origin climatology in Baker et al., 2010 & 2013 indicated by red box and red '×' respectively. Fig. prepared using Ocean Data View (Schlitzer, R., Ocean Data View, http://odv.awi.de, 2014).

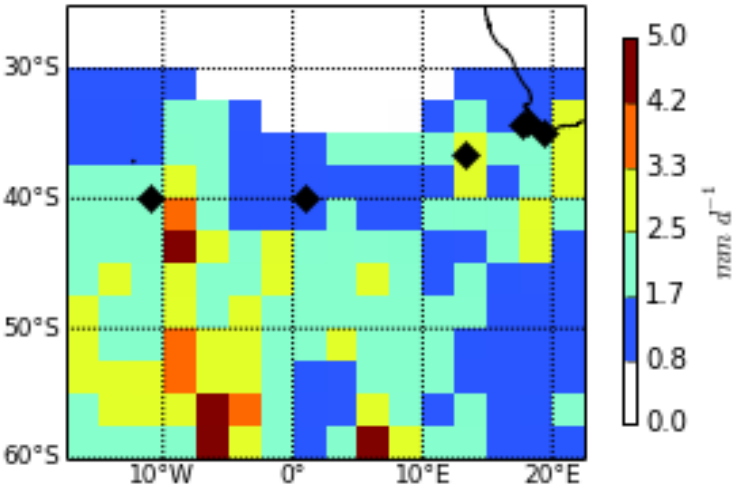

Fig. 2. Rain sample locations (◆) and average long-term monthly mean precipitation rates for the months October to January. CMAP Precipitation data was obtained from NOAA/OAR/ESRL PSD, Boulder, Colorado, USA, via the online portal at http://www.esrl.noaa.gov/psd/ (Xie, P., and P.A. Arkin, 1997).

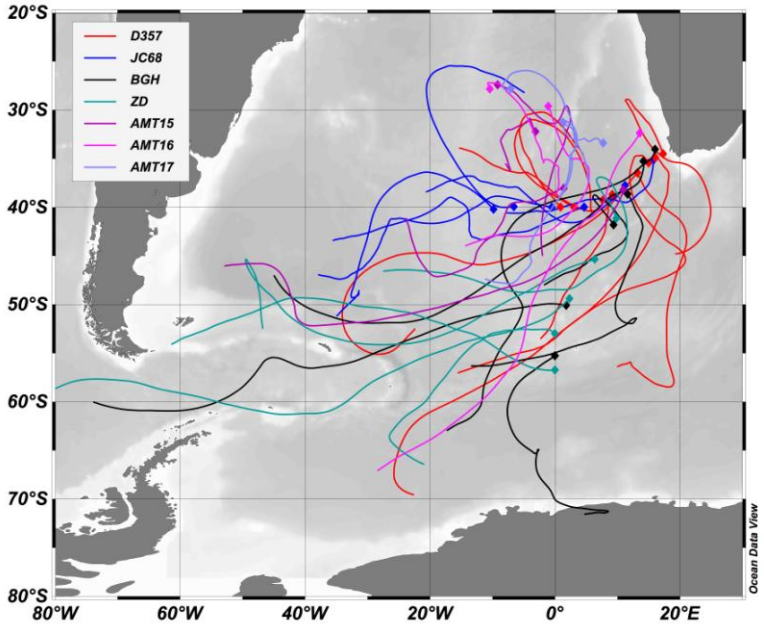

Fig 3. Typical air mass back trajectory simulations for each aerosol sample, coloured according to cruise. Back trajectories produced using the HYSPLIT model using a 10 m arrival height (Draxler and Rolph; http://www.arl.noaa.gov/HYSPLIT.php). Figure prepared using Ocean Data View (Schlitzer, R., Ocean Data View, http://odv.awi.de, 2014).

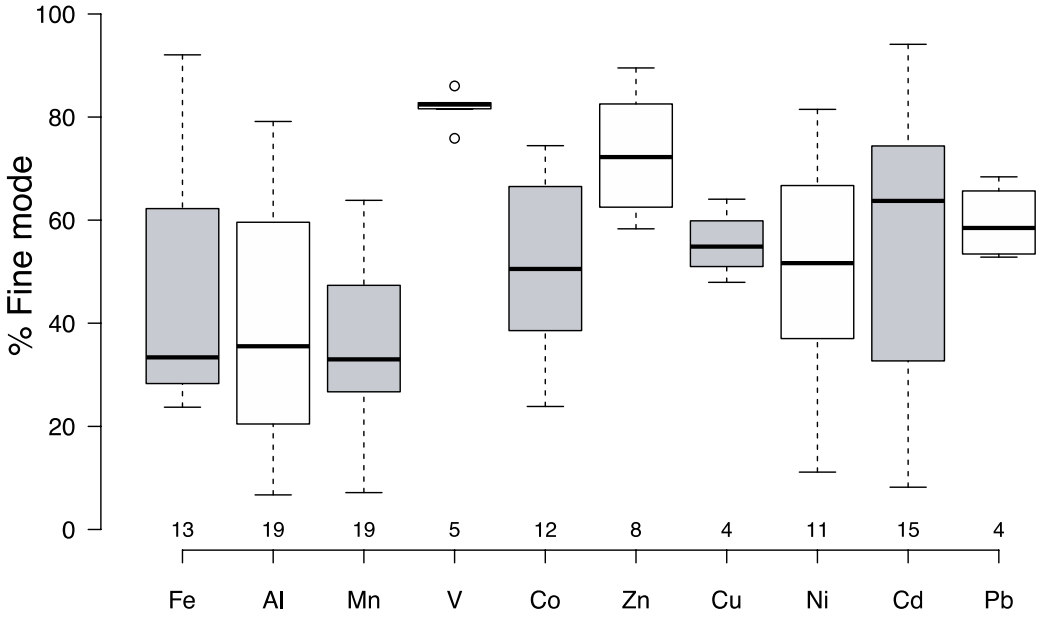

Fig. 4. Box and whisker plot showing percentage contribution of the fine mode (<1 μm particles) to overall soluble trace metal concentrations, for samples where amounts in both coarse and fine mode were above the limit of detection. The number of data points for each element is shown below each box. Centre lines show the medians, box limits show the interquartile range, whiskers extend to data points that are within 1.5 x the interquartile range of the upper or lower quartile, and dots show outliers. Fig. produced using BoxPlotR (http://boxplot.tyerslab.com/).

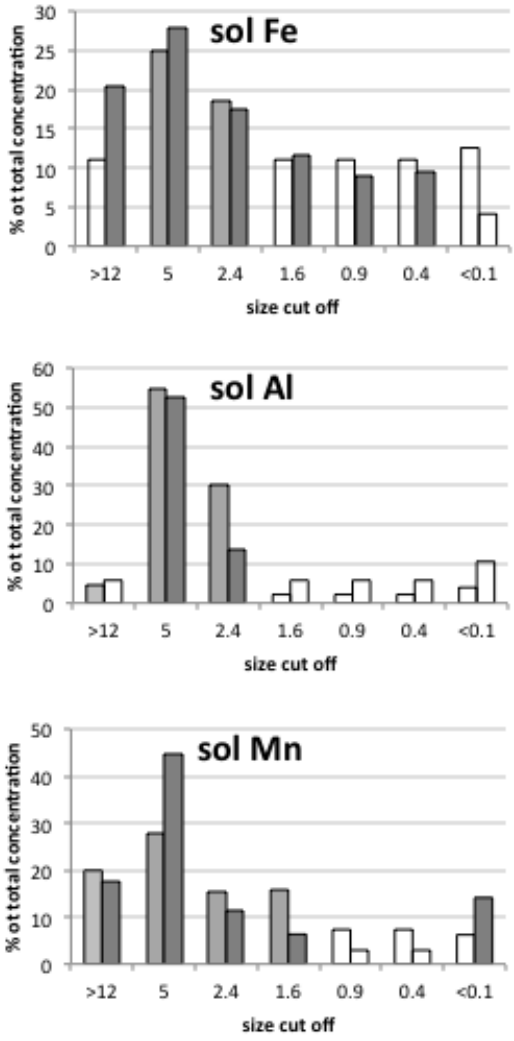

Fig. 5. Size distribution of soluble Fe (A), Al (B) and Mn (C) in two samples collected using a multistage impactor during cruise D357. Unshaded bars indicate measurements below the limit of detection.

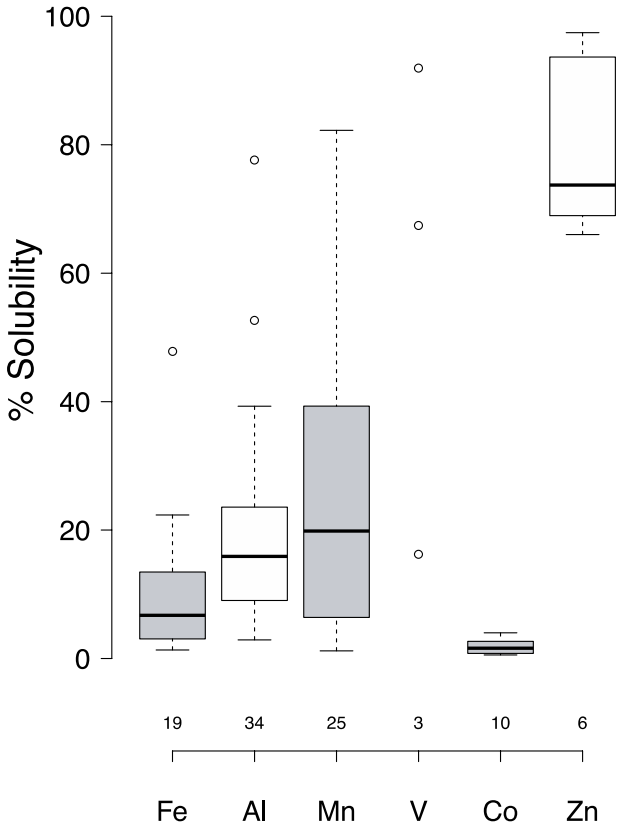

Fig. 6. Box and whisker plot showing trace metal % solubility in samples where both total and soluble concentrations were above the limit of detection. Details of the plot as for Fig. 4.

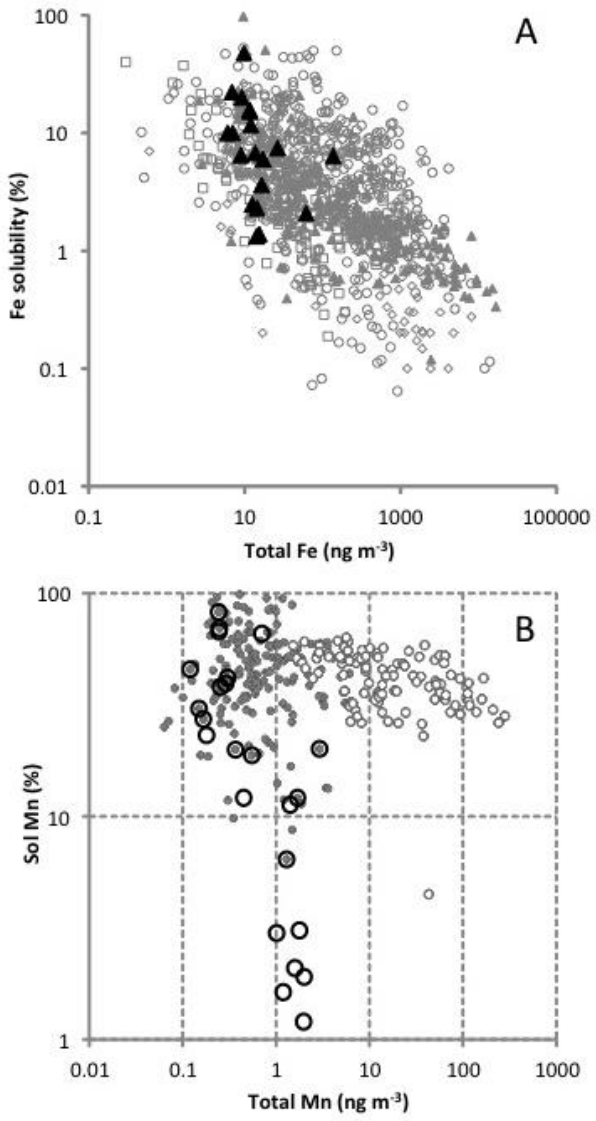

Fig. 7. Percentage solubility plotted against total atmospheric concentration of aerosol Fe (A) and Mn (B). In A, the South East Atlantic data set (▲) is superimposed on the global data set reported by Sholkovitz et al., 2012 (grey symbols). Symbol type indicates the extraction solvent used as follows: ○ = deionised water; ▲ = ammonium acetate; □ = formate buffer; ◇ = seawater. (B). In B, the South East Atlantic data set (○) is superimposed on the Atlantic data set reported by Baker et al., 2014 (grey symbols), divided into Saharan (○) and non-Saharan samples (◆).

Tables

Table 1. Dates of cruises included in this compilation.

Cruise	Full name	Sampling dates	Number of samples	
			Aerosol	*Rain*
AMT 15[a]	Atlantic Meridional Transect 15	19 - 25 October 2004	3	-
AMT 16[a]	Atlantic Meridional Transect 16	22 - 27 May 2005	3	-
AMT 17[a]	Atlantic Meridional Transect 17	19 - 23 November 2005	3	-
ZD[b]	ANTXXIV/3 (GIPY5, Zero & Drake)	12 - 21 February 2008	5	-
BGH[b,c,d]	MD166 BONUS-Good Hope	14 February - 12 March 2008	7	-
D357	Geotraces section GA10	18 October - 19 November 2010	11	4
JC68	Geotraces section GA10	28 December 2011 - 7 January 2012	6	2

a. Fe, Al and Mn concentrations included in Baker et al., 2013.

b. Fe concentrations included in global compilation of Sholkovitz et al., 2012

c. Mn, Cu, Pb and Cd concentrations included in Boye et al., 2012.

d. Co dry deposition flux range included in Bown et al., 2011.

Table 2. Median and range of aerosol total metal concentrations ($C_{atm, total}$) samples, number of observations (n), number of observations above the limit of detection (n>LoD), and average ± standard deviation enrichment factors (EF) relative to shale. All concentrations are corrected for the procedural blank. Median and EF calculation treats upper limit estimates for samples below the LoD as exact concentrations; Max gives the maximum fully quantified value.

	$C_{atm, total}$ (pmol m^{-3})			**n**	**EF**
	Median	***Min***	***Max***	**(n>LoD)**	***Average***
Fe	206	< 25	2438	39 (20)	2.2 ± 2.6
Al	346	139	7343	36 (35)	n/a
Mn	5	< 1	53	32 (25)	8 ± 12
V	3	< 0.3	4.2[a]	13 (4)	10 ± 8
Co	1	< 0.1	4	17 (10)	66 ± 79
Zn	11	< 3	92	17 (6)	148 ± 197

a. The maximum upper limit for total V was <11 pmol m^{-3}

Table 3. Median, range, first and third quartiles (*Q1* and *Q3*) of aerosol soluble metal concentrations ($C_{atm,\ soluble}$) samples, number of observations (n) and number of observations above the limit of detection (n>LoD). All concentrations are corrected for the procedural blank. Median, Q1 and Q3 calculations treat the upper limit estimates for samples below the LoD as exact concentrations.

	$C_{atm,soluble}$ (pmol m^{-3})					**n (n>LoD)**
	Median	***Min***	***Max***	***Q1***	***Q3***	
Fe	6	< 2.6	156	4.0	16	39 (33)
Al	55	< 2.6	885	33	131	36 (35)
Mn	1.2	0.35	11	0.8	2.4	32 (31)
V	0.7	< 0.19	3.0	0.43	1.0	18 (11)
Co	0.06	< 0.01	1.66	0.02	0.22	29 (27)
Zn	24	< 6.3	541	17	67	39 (31)
Cu	2	0.8	17	1.65	4.87	24 (23)
Ni	1	< 0.36	7.1	0.55	1.45	17 (14)
Cd	0.05	< 0.01	0.14	0.02	0.07	24 (17)
Pb	0.36	0.1	2.04	0.25	0.5	28 (26)

Table 4. Dry deposition fluxes for soluble and total trace metals, calculated on a per sample basis. Fluxes have been calculated using a single deposition velocity (V_d) for all elements, and by using larger and smaller values of V_d for elements expected to be primarily in the coarse and fine mode respectively (see text for details). Median calculation treats upper limit estimates for samples below the LoD as exact concentrations; Max gives the maximum fully quantified value. Results are not given for total Cu, Ni and Cd as all samples were <LoD.

		$F_{dry,}$ (nmol m^{-2} day^{-1})							
		Soluble				**Total**			
	V_d (cm s^{-1})	***Median***	***Min***	***Max***	***n***	***Median***	***Min***	***Max***	***n***
Fe	1	5.2	<2.3	135	39	178	<21.6	2106	39
	0.3	1.6	<0.7	40		53	<6.5	632	
Al	1	48	<2.3	764	36	299	120	6344	36
	0.3	14	<0.7	229		90	36	1903	
Mn	1	1.0	0.3	9.2	32	4.3	<0.8	46	32
	0.3	0.3	0.1	2.8		1.3	<0.3	13.8	
V	0.3	0.2	< 0.05	0.8	18	0.9	<0.07	1.1[a]	13
	0.03	0.02	<0.005	0.08		0.09	<0.007	0.11	
Co	1	0.05	0.01	1.4	29	0.6	<0.07	3.6	17
	0.3	0.02	0.003	0.43		0.2	<0.02	1.09	
Zn	0.3	6	<1.6	140	39	2.9	<0.9	24	17
	0.03	0.6	<0.16	14		0.29	<0.09	2.4	
Cu	0.3	0.6	0.2	4.4	24	-	-	-	-
	0.03	0.06	0.02	0.44					
Ni	0.3	0.26	0.1	1.9	17	-	-	-	-
	0.03	0.026	0.01	0.19					
Cd	0.3	0.01	0.003	0.04	24	-	-	-	-
	0.03	0.001	0.003	0.004					
Pb	0.3	0.09	0.03	0.53	29	-	-	-	-
	0.03	0.009	0.003	0.053					

a. The maximum upper limit for total V was <2.8 nmol m^{-2} d^{-1} using V_d of 0.3 cm s^{-1} and <0.28 nmol m^{-2} d^{-1} using V_d of 0.3 cm s^{-1}

Table 5. Volume weighted mean (VWM) and range of rainwater trace metal concentrations, average enrichment factors (EF) and wet deposition fluxes (F_{wet}) calculated using areally averaged precipitation rates across 36-40^{o}S and 11 ^{o}W - 16^{o}E for October - January. Error on F_{wet} calculated by propagation of weighted standard deviations of the rainwater concentration and precipitation rate. For elements indicated *, some samples were below the LoD, and so have been given a substitute value of < 0.75 x the LoD (see Section 2.3 of the main text); the EF and flux values are considered upper limits in these cases.

	C_{rain}, (nmol L^{-1})				**EF**	**F_{wet}, (nmol m^{-2} d^{-1})**
	VWM	***Min***	***Max***	***N (n> LoD)***	***Average***	
Fe	704	170.0	1711.1	6 (6)	4	1007 ± 1203
Al	792	349.0	1905.9	6 (6)	-	1132 ± 1043
Mn	32	13.2	75.7	6 (6)	8	46 ± 46
V*	<10	<6.1	15.1	6 (2)	16	14 ± 11
Zn	686	291.8	1798.0	6 (6)	1793	981 ± 1006
Co	3.2	1.6	8.2	4 (4)	26	4.6 ± 4.7
Ni*	<0.02	<0.01	0.03	4 (1)	0.05	0.03 ± 0.02
Cu*	<25	12	12[a]	4 (1)	116	35 ± 29
Cd*	<0.3	<0.1	1.1	4 (1)	397	0.5 ± 0.6
Pb	9.7	4.0	16.5	4 (4)	297	14 ± 12

a. The maximum upper limit for Cu was <45 nmol L^{-1}

SUPPLEMENTARY INFORMATION

Atmospheric trace metal concentrations, solubility and deposition fluxes in remote marine air over the south-east Atlantic

Rosie Chance[a,*], *Timothy D. Jickells*[a], *Alex R. Baker*[a],

a. Centre for Ocean and Atmospheric Sciences, School of Environmental Sciences, University of East Anglia, Norwich, NR4 7TJ, UK.

** Corresponding author. Current address: Wolfson Atmospheric Chemistry Laboratory, Department of Chemistry, University of York, YO10 4DD, UK.*

Email address: rosie.chance@york.ac.uk

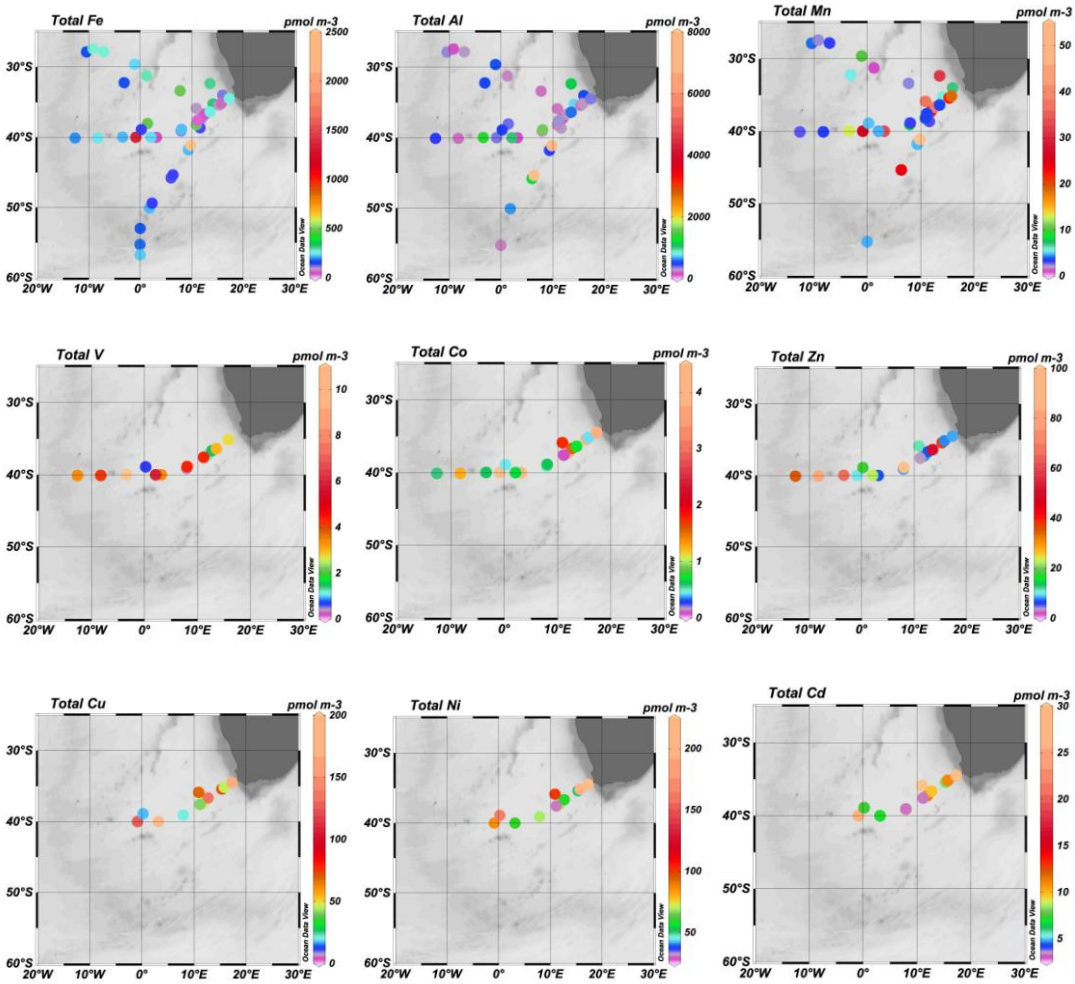

Figure S1. Atmospheric aerosol total metal concentrations included in the data compilation. Figure prepared using Ocean Data View (Schlitzer, R., Ocean Data View, http://odv.awi.de, 2014).

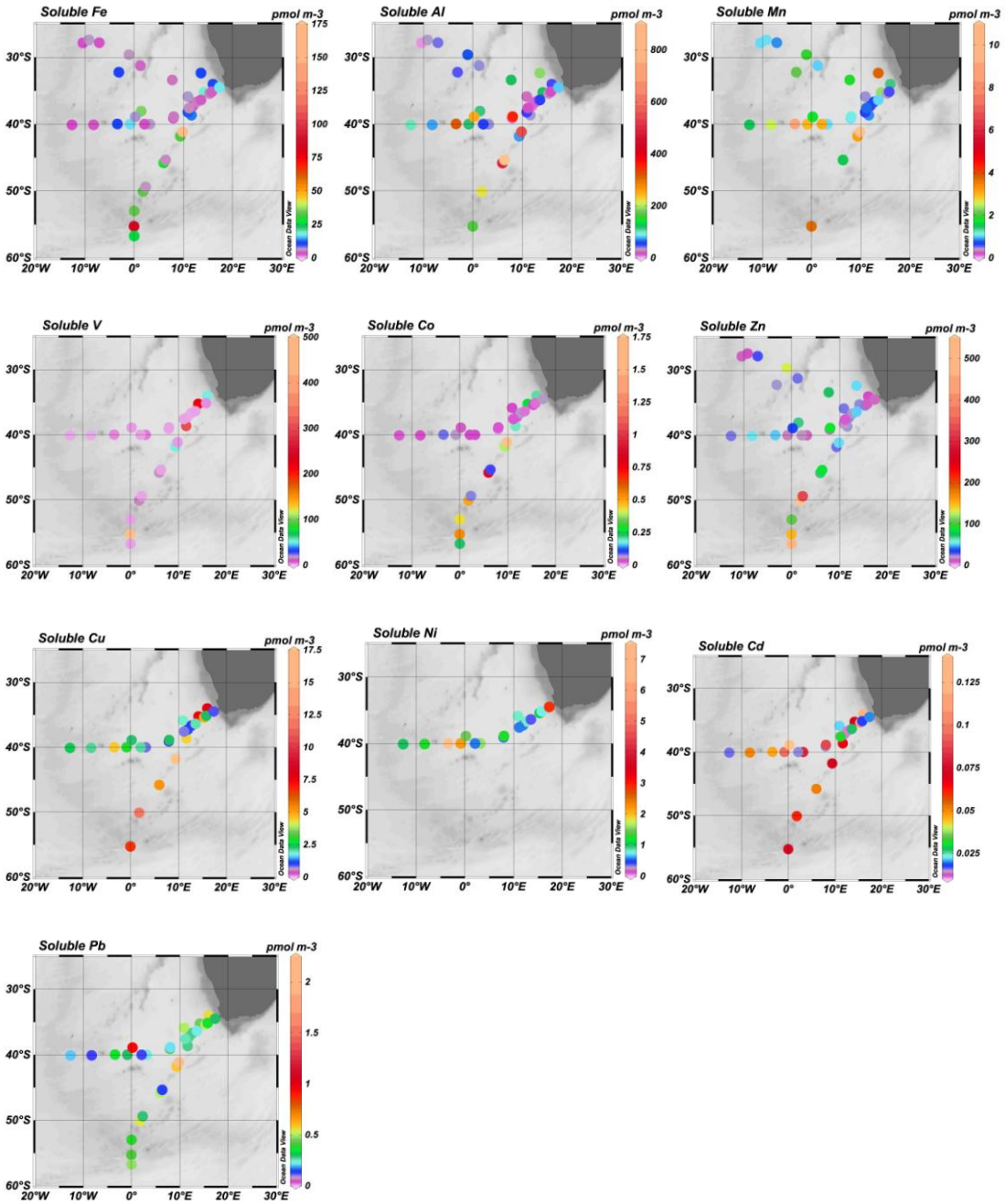

Figure S2. Atmospheric aerosol soluble metal concentrations included in the data compilation. Figure prepared using Ocean Data View (Schlitzer, R., Ocean Data View, http://odv.awi.de, 2014).

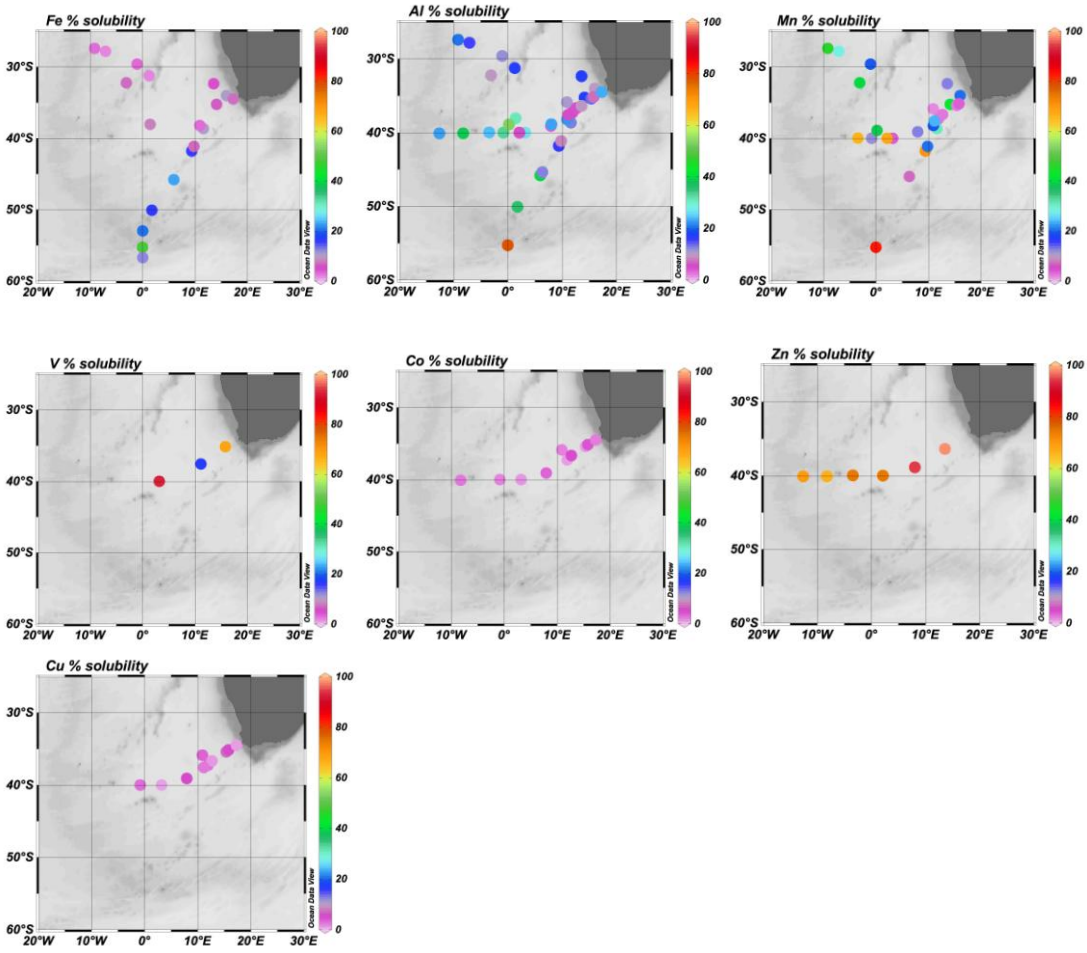

Figure S3. Atmospheric aerosol percentage solubility included in the data compilation. Figure prepared using Ocean Data View (Schlitzer, R., Ocean Data View, http://odv.awi.de, 2014).

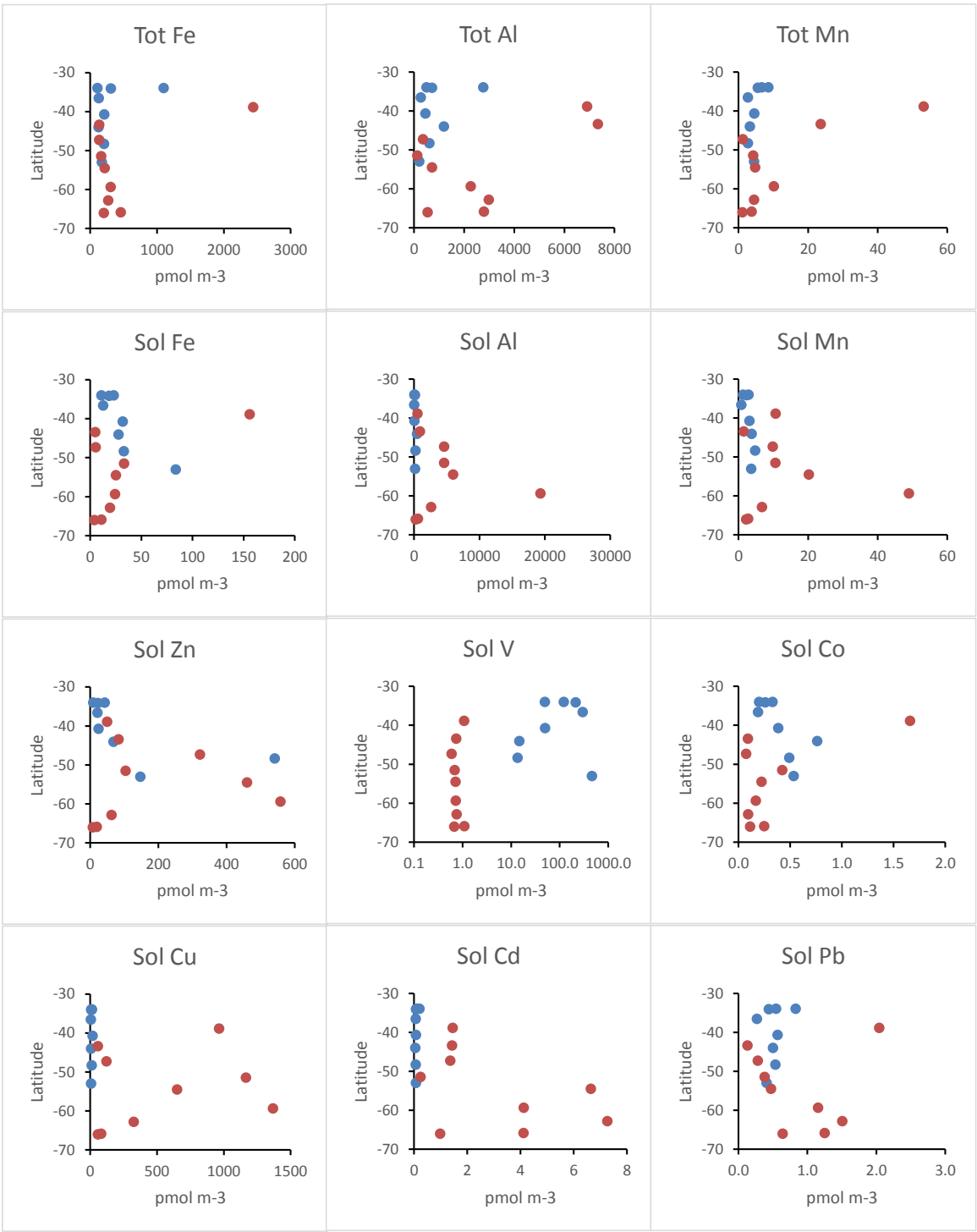

Fig. S4. Trace metal concentration plotted by latitude for the BGH (blue dots) and ZD (red dots) cruises.

Table S1. Details of rain sampling events. *These samples were collected over longer periods due to on-going drizzle with intermittent bouts of light rain.

Sample	Date	Time (UT)	Latitude (°S)	Longitude (°E)	Sampling duration (hrs)	Volume (mL)
D357 R01	22/10/2010	20:25	36°31.9'	13°32.9'	0.83	10
D357 R02	30/10/2010	17:15	39°59.7'	00°51.3	1.17	20
D357 R03	08/11/2010	15:20	34°02.0'	18°09.6	0.92	15
D357 R05	19/11/2010	19:50	34°18.2	17°34.7	14.83*	20
JC68 R01	26/12/2011	07:45	34°56.9'	19°20.8	4.75	50
JC68 R03	07/01/2012	20:55	40°00.1'	10°57.9'	9.75*	35

Table S2. Analytical limits of detection (pmol m^{-3}) for total and soluble trace metal concentrations for aerosol samples collected during this study, calculated using the average air sample volume for each cruise and the LoD. The procedural LoD was used except where filter blanks were below the analytical LoD, in which case values are calculated from the analytical LoD. Values are given for back-up (b) and slotted (s) filters, or the two combined where size segregated samples were collected, n.d. indicates parameter was not measured.

Cruise	Average air volume, m3	Sample type	Fe	Al	Mn	V	Co	Zn	Cu	Ni	Cd	Pb
							Total concentration, pmol m^{-3}					
AMT 15	2225	b + s	144	108	1							
AMT 16	2931	b	110	41	4							
AMT 17	2180	b + s	197	133	2							
ZD	3775	b	3	126	1							
BGH	4174	b	3	30	1							
D357	2568	b + s	71	20	1	0.3	0.2	9.4	8.9	85	3.9	n.d.
JC68	2677	b + s	287	38	4	0.5	0.8	7.9	n.d.	n.d.	n.d.	n.d
							Soluble concentration, pmol m^{-3}					
AMT 15	2225	b	0.8	6.7	0.29			10.9				
		s	0.9	1.8	0.31			1.8				
AMT 16	2931	b	0.8	5.2	0.14			17.5				
AMT 17	2180	b	2.5	7.8	0.23			13.9				
		s	2.1	2.8	0.19			10.0				
ZD	3775	b	0.2	8.6	0.08	0.4	0.079	6.3	0.5		0.079	0.19
BGH	4174	b	0.4	8.3	0.12	0.4	0.072	6.9	0.4		0.072	0.07
D357	2568	b	0.6	1.6	0.04	0.1	0.003	4.7	0.2	0.5	0.002	0.03
		s	0.3	2.9	0.05	0.1	0.003	9.8	0.7	0.1	0.002	0.3
JC68	2677	b	2.2	5.1	0.07	0.09	0.005	3.1	0.3	0.1	0.005	0.02
		s	2.1	1.3	0.02	0.09	0.002	5.9	1.5	0.1	0.001	0.05

Table S3. Examples of previously reported total and soluble trace metal concentrations in marine aerosols, selected for comparison with this work, and ranges of concentrations reported in this work. Where available, ranges or median values (marked *) are given; ~ indicates summary value given in reference; < indicates values below LoD.

Ref.	Region	Fe	Al	Mn	V	Co	Zn	Cu	Ni	Cd	Pb
						Total concentration, pmol m^{-3}					
This work	S. Atlantic	<25 - 2438	139 - 7343	<1 - 53	<0.3 - <11	<0.1 - 4	<3 - 92	< 176	<204	<29	-
A	S. Atlantic	140 - 360	1200	20							
B	S. Atlantic	36.3 - 1450	154 - 2260	0.8 - 27							
C	S. Atlantic	21 - 5900									
D	S. Atlantic	47 - 18684					7 - 2654', 60	0.9 - 171, 3.3*	0.9 - 10, 2.2*	0.02 - 3.7, 0.1*	0.3 - 7.3, 1.1
E	S. Atlantic	100							2.7	7.2	14
F	S. Ocean (Indian sector)	180 - 680									
G	S. Ocean (Indian sector)	12 - 201									
H	Pacific		567*	5*							
I	Pacific				~0.7	~0.05	~1.4	~1.3		~0.14	
J	Pacific				0.4 - 15						
	N. Atlantic				0.8 - 13						
K	NW. Atlantic				≤ 275						
L	NW. Atlantic					0.09 - 18					
M	N. Atlantic & N. Pacific							0.3 - 16			
						Soluble concentration, pmol m^{-3}					
This work	S. Atlantic	<2.6 - 156	<2.6 - 885	0.35 - 11	<0.19 - 3.0	<0.01 - 1.66	<6.3 - 541	0.8 - 17	<0.36 - 7.1	<0.01 - 0.14	0.1 - 2.04
B	S. Atlantic	2.4 - 49.3	28 - 214	0.3 - 23.9							
F	S. Ocean (Indian sector)	2 - 48									
L	NW. Atlantic					0.05 - 1.76					
N	S. Atlantic						10.4 - 68.6	5.3 - 22.2	1 - 4.4	0.04 - 0.18	0.7 - 8.7

References: A - Losno et al., 1992; B - Baker et al., 2013; C - Radlein & Heumann, 1992; D - Volkening & Heumann, 1990; E - Radlein & Heumann, 1995; F - Gao et al., 2013; G - Heimburger et al., 2012; H - Guieu et al., 1994; I - Arimoto et al., 1990; J - Duce & Hoffman, 1976; K- Duce et al., 1975; L - Shelley et al., 2012; M - Paytan et al., 2009; N - Witt et al., 2006.

***Research Highlights**

- Aerosols and rainwater were collected in the south-east Atlantic
- Total concentrations of Fe, Al, Mn, V, Co and Zn were measured
- Soluble concentrations of Fe, Al, Mn, V, Co, Zn, Cu, Ni, Cd and Pb were measured
- Fractional solubilities (using pH4.7 leach) were similar to those found previously
- Wet deposition was the dominant contributor to total deposition in almost all cases